Environmental Science
Water Research & Technology

ROYAL SOCIETY OF CHEMISTRY

PAPER

View Article Online
View Journal | View Issue

Cite this: *Environ. Sci.: Water Res. Technol.*, 2022, **8**, 1092

The regenerative role of biofilm in the removal of pesticides from stormwater in biochar-amended biofilters†

Andrea C. Portmann, [a] Gregory H. LeFevre, [b] Rennosuke Hankawa, [a] David Werner[c] and Christopher P. Higgins *[a]

Low-impact, green infrastructure systems such as biofilters, particularly when amended with biochar, can help address chemical pollution conveyed *via* stormwater that is increasingly posing a threat to aquatic ecosystems and groundwater quality. Although removal of organic contaminants including pesticides by biochar-amended systems has been studied, the role of a biofouling layer on contaminant removal, biotransformation, and filter lifetime remains poorly understood. This study evaluated the removal of the pesticides atrazine, imidacloprid, and clothianidin in biologically active biochar-amended columns through complete exhaustion of contaminant removal capacity. The resultant data indicate that biological processes accounted for 20–36% of overall removal in the biochar-amended sand columns. In addition, a combined target and suspect screening approach using liquid chromatography quadrupole time-of-flight mass spectrometry (LC-QToF-MS) was employed to evaluate the potential transformation of these three pesticides and release of the transformation products (TPs). All TPs detected in the effluent remained below 2.5% of their respective parent influent concentrations for the duration of the experiment. Furthermore, at a biochar application rate of 0.5 wt%, the presence of an active biofilm prolonged the filter lifetime by 1.8–2.3 times compared to a fouled but inactive filter, where removal was presumably dominated by adsorption only. Scenario modelling estimates showed that biochar-amended biofilters could last at least 17 years before exceeding aquatic life threshold values at biochar-application rates as low as 1 wt% (5 vol%) in a representative case study. Results of this study provide novel insight on pesticide TP formation in biochar-amended biofilters and estimation of filter lifetimes.

Received 24th November 2021,
Accepted 21st March 2022

DOI: 10.1039/d1ew00870f

rsc.li/es-water

Water impact

Exhaustion of black carbon media in stormwater biofilters remains a major hurdle for the wide implementation of this cost-effective and sustainable stormwater treatment technology. This study shows that biologically active biochar-amended stormwater filters improve removal of pesticides. Our results indicate that the combined presence of biochar and biofilm leads to a prolonged filter lifetime.

1. Introduction

Harnessing alternative water resources such as stormwater through capture and treatment is a promising strategy to help address both water scarcity and contamination.[1–3] Nevertheless, to make stormwater runoff a viable and safe water resource, effective methods for water quality improvements are essential. In recent years, the implementation of green infrastructure systems and stormwater control measures (SCMs) has gained attention among practitioners, especially the use of infiltration techniques.[4] Traditionally, however, SCMs have focused on flow reduction and water capture but have not been designed for water quality improvement.[4,5] Contamination of urban streams with trace organic contaminants (TOrCs) stemming from stormwater runoff such as polycyclic aromatic hydrocarbons (PAHs),[5–7] pesticides,[5,6,8–11] vehicle-associated compounds,[12] flame retardants,[7,11] and pharmaceuticals[7,11,13] may lead to substantial aquatic health impacts such as acute/chronic toxicity[14–17] and endocrine disruption,[18,19] surface

[a] *Department of Civil & Environmental Engineering, Colorado School of Mines, Golden, Colorado 80401, USA. E-mail: chiggins@mines.edu; Tel: +720 984 2116*
[b] *Department of Civil & Environmental Engineering, IIHR-Hydroscience & Engineering, University of Iowa, Iowa City, IA 52242, USA*
[c] *School of Engineering, Newcastle University, Newcastle upon Tyne, NE1 7RU, UK*
† Electronic supplementary information (ESI) available. See DOI: https://doi.org/10.1039/d1ew00870f

water quality degradation,[5] and drinking water impairments of groundwater aquifers.[20,21] During the past 20 years, decentralized biofilters or bioretention systems have been increasingly gaining traction as a viable alternative to centralized stormwater treatment systems.[22] Biofilters amended with conventional media (*i.e.*, soil, sand) are typically effective at removing suspended solids and thus particulate-bound organics (*e.g.* petroleum hydrocarbons, PAHs) with removal values commonly as high as 80–90%.[23,24] However, limited removal in conventional biofilters was observed for less hydrophobic organic contaminants[24] and our understanding of the attenuation of dissolved organic contaminants remains limited.[5] Specifically, TOrCs such as hydrophilic pesticides pose one of the greatest risks for groundwater contamination[25] due to their high mobility and low sorptive affinity towards soil and conventional infiltration media such as sand.[5,11] These findings highlight the need to modify conventional green infrastructure systems for the removal of this class of contaminants.[11,14]

In light of the challenge that dissolved and hydrophilic TOrCs pose to maintaining or improving water quality, amending stormwater treatment systems with black carbon adsorbents like biochar has become a strategy of interest to improve contaminant removal.[2,4,26] Biochar is a cost-effective means of improving the removal of hydrophilic TOrCs, as has been demonstrated in laboratory batch and column studies,[27,28] as well as in pilot-scale biofilters.[29] As the dominant abiotic removal process for TOrCs is adsorption, biochar properties such as surface area, aromaticity, and internal pore size distribution – especially microporosity and mesoporosity[27,30] – appear to control the removal of organic contaminants.[2] Depending on the functional group(s) of the target pollutant, different mechanisms can be responsible for the interaction between the organic contaminant and biochar surface: non-polar compounds attach to hydrophobic sites on the biochar surface, whereas polar compounds engage in hydrogen bonds with polar surface groups.[31] Charged organic compounds may also be retained *via* electrostatic attraction, especially cationic compounds, since most biochar surfaces are negatively charged.[31]

In addition to abiotic sorptive removal, the microbial activity of stormwater filters is thought to play an important role for TOrC attenuation.[32,33] Immobilized microbial biofilms have long been used in water and wastewater treatment[34] and also in the bioremediation of xenobiotics.[35,36] The suitability of biochar to serve as habitat and inoculum carrier for microorganisms has been described previously,[37,38] although not all literature agrees.[39] The suitability of a biochar to serve as biofilm attachment site may be highly dependent on specific properties, including surface area, hydrophobicity, water holding capacity,[37] and biochar carbon availability.[38] Further, Saquing *et al.*[40] reported that biochar can function as both electron donor and acceptor, and thus should be seen as rechargeable reservoir of bioavailable electrons, a feature which could potentially promote the biodegradation of contaminants in bioretention systems. The stimulating effect of biochar on microbial processes involving inorganics has been demonstrated for Fe(III) reduction[41] and nitrate reduction (*i.e.*, denitrification).[40] Moreover, biological degradation may act directly on biochar-bound organic contaminants,[42] which has important mechanistic implications. Furthermore, biofilm-coated biochar is reported to benefit TOrCs removal, possibly due to microbial biodegradation.[33,43] Thus, biochar-attached biofilms could facilitate sustained contaminant removal, potentially *via* a synergistic relationship between microbial degradation and biochar adsorption.[32] This process, coined bioregeneration, has been described for biologically active granular activated carbon (GAC) filters in water treatment, and implies that the sorptive capacity of adsorbents can be restored by microbial degradation freeing up sorption sites.[44]

Overall, disambiguating the contributions of individual processes on total removal is challenging, and very limited research is available on the disentangling of sorptive and biological processes in biochar-amended systems.[45,46] In practice, SCMs are often considered "black box" passive water treatment systems.[4] The design of biochar-amended biofilters is further complicated by processes that are difficult to simulate in the laboratory but inherently arise in field-scale systems, such as the impact of variable saturation conditions, clogging, or biofouling on biochar sorption. For instance, the addition of an external carbon source (*e.g.* woodchips, compost, humic acid) is known to facilitate biological processes and can benefit contaminant removal,[33,47,48] but may also lead to accelerated exhaustion of adsorption sites or pore clogging and concomitant biochar aging.[49,50] Generally, there are only a few studies providing insight into long-term performance of biochar-amended stormwater treatment systems.[22] Thus, a better understanding of the effect of an active microbial biofilm (*i.e.*, biodegradation) on overall TOrC removal over one full lifetime of a biofilter is warranted to inform design, maintenance, lifetime, and risk assessment (*e.g.*, toxicity of metabolites) of biochar-amended SCM systems. Moreover, inclusion of transformation products (TPs) in the analysis of biochar-amended biofilter effluents is lacking in the literature, even though TPs of pesticides are a concern and increasingly found in drinking water sources[51] and in groundwater – sometimes at higher concentrations than their parent compounds.[21] Thus, it is essential to determine if biochar-amended biofilters could be a potential source of TPs into the environment. As biodegradation in biofilm–biochar filters may potentially prolong biofilter lifetime in the long term, the primary objectives of this study were to: i) assess the role of biofilm in overall pesticide removal in biochar-amended biofilters and determine the relative importance of biodegradation compared to sorption; ii) evaluate the effect of the combined biofilm–biochar presence and thus biodegradation on filter lifetime; and iii) elucidate the main transformation pathways of select pesticides occurring in biotic biochar–sand systems compared to controls. To address these objectives, we studied

the removal and transformation of atrazine, imidacloprid, and clothianidin in laboratory-scale biochar-amended sand columns over four months and compared the findings to results from inhibited (*i.e.*, inactivated biofilm) biochar–sand columns and sand-only columns (both biotic and inhibited). Hydrophilic pesticides, including atrazine and neonicotinoids, are increasingly being discovered in urban stormwater.[13] Our decision to study neonicotinoids in biochar-amended biofilters was based on their emerging nature and lack of environmental research data (personal communication by the California Department of Pesticide Regulation). The resultant column breakthrough curves of the three pesticides were used to estimate parameters of a contaminant transport model to simulate representative biofilter lifetimes in different case study scenarios.

2. Methods

2.1. TOrCs analysis

The TOrCs suite selected for target analysis in this study included the parent compounds atrazine, imidacloprid, and clothianidin. TPs also targeted for analysis included desethylatrazine (DEA), desisopropylatrazine (DIA), 2-hydroxy-atrazine (OH-ATZ), desnitro-imidacloprid (desnitro-IMI), imidacloprid-urea (IMI-urea), imidacloprid–olefin (IMI–olefin), and 6-chloronicotinic acid (6-CNA). Analytical standards for TPs of clothianidin were not commercially available and therefore not included in the target analysis. Isotope dilution was conducted using the surrogate standards atrazine-d_5, imidacloprid-d_4, and clothianidin-d_3. Information and details on source and purity of analytical standards (natives and surrogates) can be found in the ESI,† Table S1. Literature-derived microbial transformation pathways for atrazine, imidacloprid, and clothianidin can be found in Fig. S1–S3.† Concentrations of TOrCs in aqueous samples were quantified by liquid chromatography quadrupole time-of-flight mass spectrometry (LC-QToF-MS) using a SCIEX ExionLC™ high-pressure liquid chromatography (HPLC) system equipped with a biphenyl analytical column (3 μm, 100 × 3 mm; Phenomenex, Torrance, CA), coupled to a SCIEX X500R QToF-MS system (Framingham, MA) using electrospray ionization in positive mode (ESI+) with SWATH® data-independent acquisition for both ToFMS and MS/MS mode. Details on the MS parameters and LC conditions can be found in the ESI.†

2.1.1. Target analysis. Target analytes were identified based on precursor accurate mass (mass error <10 ppm), isotopic pattern (isotopic ratio error <40%), and retention time (ΔRT <0.05 min) compared to analytical (native) standards, and quantified using calibration standards in the range of 0.005 μg L^{-1} to 25 μg L^{-1}. Surrogate concentrations in calibration standards (and samples) were 0.4 μg L^{-1} for atrazine-d_5 and 0.8 μg L^{-1} for both imidacloprid-d_4 and clothianidin-d_3. Accuracy of calibration standards was required to be within ±30% and the calibration curve had to be linear ($R \geq 0.99$). The limit of quantitation (LOQ) for most analytes was between 0.005 μg L^{-1} and 0.01 μg L^{-1}, except for 6-CNA, for which the LOQ was 0.05 μg L^{-1}. Considerably lower sensitivity of 6-CNA in LC-MS analysis compared to other neonicotinoid compounds has been reported previously.[52,53] Table S2† contains the LC-QToF-MS parameters for each target analyte; specifically, retention time, precursor accurate mass (quantitation), MS/MS fragment masses (qualitative confirmation), LOQ, and spike recovery data.

2.1.2. Suspect screening. To identify additional TPs of atrazine, imidacloprid, and clothianidin, a suspect screening approach was also employed. LC-QToF-MS data acquired in SWATH® mode was screened using a custom extracted ion chromatogram (XIC) list (Table S3†) containing molecular formulas and accurate masses for TPs identified using the EAWAG Biocatalysis/Biodegradation Database and Pathway Prediction System (EAWAG-BBD/PPS; **https://eawag-bbd.ethz.ch/index.html**) and a review of extant literature (Fig. S1–S3†). Identification of unknown pesticide TPs was based on accurate mass measurement for the molecular ion, isotopic pattern matching scores, and verification of MS/MS spectra. Samples were screened by searching for the protonated molecular ion $[M + H]^+$ using an XIC window of 0.02 Da, a signal to noise threshold of 10 : 1, and a noise percentage of 90%. For additional analyte confirmation, acquired MS/MS spectra were compared to fragment masses previously reported in literature (Table S2†). Suspects were confirmed by identification of at least one unique product ion accurate mass that matched known fragments (mass error <10 ppm). In a first screening of the data, only matches with precursor ion mass error <5 ppm and isotopic pattern error <40% were considered for subsequent MS/MS fragment analysis. The precursor mass error criterion was chosen to be more restrictive than the target analysis because of the absence of analytical standards. A confidence level was assigned to each suspect compound on the basis of the Schymanski scale.[54]

2.2. Materials

2.2.1. Biochar. The biochar used in this study was Mountain Crest Gardens biochar (MCG-biochar) produced by high temperature (>1100 °C) gasification of pinewood (Gropro, Inc., Etna, CA) and was selected for this study due to its superior TOrC removal performance in laboratory-scale[27,28] and pilot-scale biofilters treating stormwater.[47] The biochar was sieved to a particle size range of 53–250 μm, rinsed by deionized (DI) water, and subsequently allowed to air dry. The standard laboratory sand was of uniform particle size (210–297 μm; Sigma-Aldrich) and was used as received. Additional details related to surface area analysis and pore-size characterization of the biochar is provided in the ESI.†

2.2.2. Dissolved organic carbon (DOC) extract solutions. All experiments (batch sorption, column, and microcosm experiments) were conducted with representative synthetic stormwater based on a recipe from Grebel *et al.*[55] Dissolved organic carbon (DOC) was added from DOC extract solutions obtained by infusing local creek water with grass, leaves, and

compost over several weeks based on a recipe described elsewhere.[33] DOC obtained from natural carbon sources provides a more complex DOC source for microbial growth than from single sources (*e.g.*, humic acid) and is thought to be more representative of actual field conditions. Details on the preparation of the DOC extract solutions can be found in the ESI.†

2.2.3. Microbial enrichment solutions. Microbial enrichment solutions for column inoculation were prepared following a modified procedure described elsewhere.[33] In brief, a sediment-creek water slurry was obtained from a local creek (Clear Creek, Golden, CO) and served as the inoculum to the enrichment solutions. The same DOC extract that was used for batch and column experiments was used as growth media for the enrichment solutions. Microbial cultures for the enrichment solutions were grown over two stages of three successive inoculation–incubation cycles. Further details on the microbial enrichment procedure can be found in the ESI.†

2.3. Batch sorption experiments

Isotherm and kinetic batch experiments were carried out in 250 mL amber glass bottles (Qorpak; Clinton, PA) with representative synthetic stormwater. Batch experiments were conducted following the method described in Ulrich *et al.*[27] Briefly, after amber glass bottles were autoclaved at 135 °C for 25 min, 200 mL of representative synthetic stormwater (including 100 mg L^{-1} sodium azide) and 3.8 ± 0.3 mg of fresh MCG biochar were added to each bottle. The batches were placed on a shaker table overnight to allow for pre-equilibration of the biochar with DOC. The following day, batches were spiked with a mixture of the native parent TOrC solution using a methanol carrier (less than 0.05% of total volume), which marked time zero of the batch experiments. Isotherm batch tests were carried out in triplicates at five different initial concentrations (C_0 = 3, 10, 20, 50, and 100 μg L^{-1} for each TOrC individually) and including controls (no biochar) to account for abiotic losses of TOrCs. Samples were taken in the beginning (t = 1.5 h) from controls only and at the end (t = 92 d) from biochar batches and controls. Samples (2 mL) were taken after 0.5 hours of settling using sterile pipet tips and were transferred into glass centrifuge vials (Kimble Chase; Rockwood, TN/DWK Life Sciences, LLC). After addition of a surrogate solution in methanol (10% of final volume), vials were centrifuged at 2600 rcf for 18 min to spin down potential biochar particles. The supernatant was transferred to amber storage vials and stored at 4 °C until analysis. Kinetic batch tests were carried out with the serial method following OECD guidelines 106 (OECD, 2000) using an initial TOrC concentration of 10 μg L^{-1} (for each TOrC individually). TOrCs sampling was performed at 1.5 h, 1 d, 3 d, 7 d, 15 d, 29 d, and 67 d and the sample preparation and storage followed the same procedure as for isotherm batches.

Best-fit parameters of the Freundlich and Langmuir isotherms were obtained from the equilibrium sorption data using non-linear regression with relative weighting ($1/Y^2$) in GraphPad Prism (version 9.1.1); the corresponding figures can be found in the ESI† (Fig. S4). Akaike's information criterion (AIC) was used to compare the goodness of fit of both sorption equations and demonstrated better fits for the Freundlich isotherm for all three parent compounds. Both the AIC and best-fit values of the non-linear Freundlich isotherm coefficient K_F and the Freundlich isotherm exponent n are reported in the ESI† (Table S4).

2.4. Column experiments

Column experiments were conducted using Kimble Chase flex-columns (2.5 × 5 cm) (DWK Life Sciences, LLC) and an effective length of 5.6 cm was dry-packed with a mixture of sand and biochar (0.5 wt%). The media mixture was fixed with glass beads and glass wool at both the inlet and outlet to prevent loss of media under flow conditions. Attachment of a biofilm on the sand-biochar media and start-up of biotic columns followed a procedure described elsewhere.[33] Columns were purged with CO_2 gas right before startup to ensure fully saturated conditions and were subsequently injected with one pore volume (PV) of microbial enrichment solution at a flow rate of 0.9 mL min^{-1}, allowed to sit overnight, and then slowly recirculated at 0.08 mL min^{-1} for 48 h to promote microbial attachment. After seeding of a biofilm, columns were conditioned with representative (un-spiked) synthetic stormwater containing 10 mg L^{-1} DOC at a flowrate of 0.21 mL min^{-1} for 23 days. During conditioning, a salt tracer test was performed using a conservative tracer KBr solution (300 mg L^{-1}) to assess mean hydraulic residence times (HRT) of the columns. Effluent samples (1 mL) were taken every 20 min, diluted with Milli-Q water and analyzed by ion chromatography (IC). Based on the salt tracer data, mean HRTs of the columns were between 90–125 min (consistent with a recent bioretention study[56]), with the variance likely due to experimental variation rather than the presence of biochar or a biofilm (see Fig. S6†). After the dissolved oxygen (DO) levels in the effluent stabilized, columns were injected with representative synthetic stormwater containing 10 mg L^{-1} DOC and 200 μg L^{-1} of each TOrC (atrazine, imidacloprid, clothianidin) for 92 days at a flowrate of 0.21 mL min^{-1}. This flow rate corresponds to an infiltration rate of 2.58 cm h^{-1} and thus meets the infiltration requirement for bioretention systems (>2 cm h^{-1}).[5] Influent reservoirs (aerated) were refreshed daily to minimize microbial growth and TOrC degradation, and the methanol of the TOrC carrier solution was evaporated under N_2 in a conical glass tube. The dried TOrC residue was redissolved and added to the influent reservoirs by repeatedly (6×) adding synthetic stormwater to the glass tube and vigorous shaking, then letting it sit for 10–15 min each time. Influents of inhibited control columns (one for sand and sand + BC each) contained 200 mg L^{-1} of sodium azide (NaN_3) for continued biofilm inactivation. Influent and effluent samples were taken regularly (on average, every 2–3 days over the course of 92 days) and preserved by filtration with Millex syringe filters

(0.22 μm, 13 mm, Durapore, PVDF membrane; Millipore Sigma) and stored at 4 °C until analysis. However, not all of these samples were submitted for TOrC analysis.

General column performance was monitored by analyzing influent and effluent samples for standard water quality parameters. DO concentrations and pH were measured twice a week during the first three weeks (column conditioning) and once a week afterwards using a portable Hach multimeter (HQ40D) and DO/pH probes. DOC and total nitrogen (TN) concentrations were measured weekly (twice a week during the first seven weeks) by a TOC-L Laboratory Total Organic Carbon Analyzer (Shimadzu), and major anions were analyzed using a Dionex ICS-900 Ion Chromatography System (Thermo Fisher Scientific). Samples were diluted with in-house Milli-Q water as necessary to meet instrument specifications and calibration ranges.

2.5. Microcosm experiments

Biotic microcosms (two replicates: M1, M2) were started in autoclaved 1000 mL Erlenmeyer flasks by combining 100 mL of DOC extract solution (~250 mg L^{-1}) with 10 mL of the same microbial seeding solution used for column inoculation. Flasks were aerobically incubated at 30 °C in the dark for two weeks (17 days). After incubation, replicates M1 and M2 were spiked with TOrCs (atrazine, imidacloprid, and clothianidin; final concentration: 400 μg L^{-1} each) by adding 140 mL of autoclaved synthetic stormwater solution (no DOC). As with the column influent solutions, the methanol of the TOrC carrier solution was evaporated under N_2 before addition to the flasks. An un-spiked control (M3) was prepared to monitor microbial growth under non-exposure conditions. In addition, an inhibited control (M4) was initiated by combining 100 mL of DOC extract solution, 10 mL of NaN_3 in Milli-Q water (final concentration: 200 mg L^{-1}) instead of the microbial enrichment solution, and 140 mL of autoclaved synthetic stormwater solution (no DOC). Unfortunately, it was not possible to maintain the inhibited control as uncontaminated over the duration of the experiment and thus it was excluded from further analysis. All flasks were shaken continuously for 369 days at room temperature and sampled regularly (weekly during the first 14 weeks, then bimonthly during the next 15 weeks, and again after six months at the end of the experiment). Sample volumes were kept as low as 0.5–1.0 mL and were prepared for storage following the same method as described for column samples. To account for evaporative water losses, microcosms were weighed before each sampling event and the appropriate volume of autoclaved Milli-Q water was added to each microcosm prior to sampling.

2.6. Transport modelling

Contaminant breakthrough data were assessed using a model in MATLAB (R2019b, MathWorks, Massachusetts, United States) describing one-dimensional solute transport in porous media assuming sorption-retarded intraparticle diffusion kinetics and a Freundlich sorption isotherm (column model variables and input parameters are listed in Tables S8 and S9†). Tortuosity (τ) was used as a fitting parameter to account for intraparticle diffusion. This model was originally designed to determine the fate and transport of organic contaminants in black carbon-amended sediments or aquifers.[57,58] Ulrich *et al.*[27] used an adapted version to demonstrate that including diffusion-limited sorption kinetics allows the prediction of TOrC breakthrough curves (BTCs) in abiotic biochar-amended sand filters based on sorption parameters derived from abiotic batch tests. The same model has been successfully employed to model the breakthrough of per- and polyfluoroalkyl substances (PFASs) in a pilot-scale GAC filtration system, even though it was found that assuming local sorption equilibrium generated a better fit to the observed data.[59] In the present study, the original model was adapted for constant influent concentration (as opposed to a pulse).

Estimation of sorption and kinetic parameters (*i.e.*, tortuosity) based on batch equilibrium and kinetic sorption data for use in column breakthrough prediction was successfully demonstrated previously;[27] however, in the current study, results were not deemed satisfactory (Fig. S16 and S17†). We assume that the presence of a biofilm layer in the porous media limited the transferability of parameters from abiotic batch studies (microbial growth inhibited by NaN_3) to biologically active flow-through systems. Best-fit Freundlich sorption (K_F, n) and kinetic parameters (τ) for each compound were therefore directly estimated based on the effluent data observed in the biotic BC + sand columns (Fig. S19†). The best-fit parameters were then used to predict TOrC breakthrough and biofilter lifetime in several case study simulations (scenarios). Assuming that the biofilter effluent were discharged into receiving surface waters, the "biofilter lifetime" or "breakthrough" was defined as the time when the effluent concentrations would exceed chronic aquatic life benchmarks specified by the European Union or the United States Environmental Protection Agency (U.S. EPA). Representative stormwater influent concentration ranges were estimated based on reported surface water data in the literature (storm- and stream water), with the corresponding maximum concentrations being used to simulate worst-case scenarios. The simulated continuous filter lifetimes were then adjusted based on a representative field-scale biofilter (infiltration basin) for a residential area in Denver, CO, receiving a representative amount of rainfall. Detailed calculations are provided in the ESI† (Table S11).

3. Results and discussion

3.1. Biological activity of columns

The average column influent DO concentration of 7.12 (±0.11) mg L^{-1} consistently decreased in the column effluent for all four tested conditions (Fig. 1a; $p = 9.10 \times 10^{-4}$, Rank-sum test, $\alpha = 0.05$), indicating continued aerobic microbial activity throughout the study. Nevertheless, DO removal was

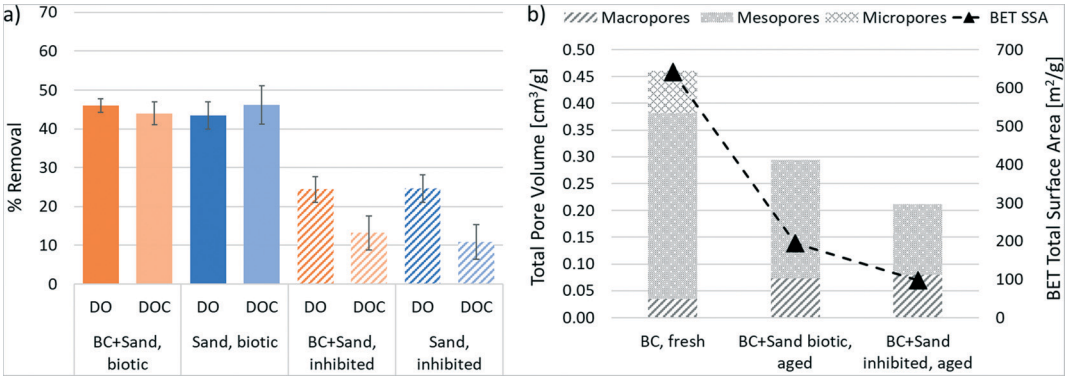

Fig. 1 a) Biological activity of columns: removal of dissolved oxygen (DO) during days 7–110 and removal of dissolved organic carbon (DOC) during days 11–103; shown are the mean and standard error of the mean (SEM) with sample sizes n = 54, 18, 18, 18, respectively. b) Effect of biofilm and ageing on biochar properties: Brunauer–Emmett–Teller specific surface area (BET SSA) and pore volume distribution of fresh MCG-biochar compared to aged biotic and inhibited samples. Ageing consisted of column conditioning with synthetic stormwater containing ~10 mg L^{-1} DOC (23 days) followed by injection of synthetic stormwater with ~10 mg L^{-1} DOC and ~200 μg L^{-1} TOrCs (92 days).

significantly greater in biotic columns (both with and without biochar) compared to inhibited conditions ($p = 1.96 \times 10^{-4}$; Wilcoxon sign rank test, $\alpha = 0.05$). Similar results occurred for removal of DOC in the columns (Fig. 1a): the overall DOC removal in the biotic systems (both sand and BC + sand) was significantly greater (45%) compared to the inhibited controls (12%; $p = 3.85 \times 10^{-6}$, paired-sample t-test, $\alpha = 0.05$). However, there was some comparably minor microbial activity in the inhibited columns, indicating that the addition of sodium azide was not sufficient to suppress all microbial activity. This is supported by the fact that the observed average DOC removal was significantly non-zero ($p = 0.0269$ and $p = 0.0086$ for sand, inhibited and BC + sand, inhibited, respectively; one-sample t-test, $\alpha = 0.05$). We believe that the term "inhibited" sufficiently reflects this circumstance (compared to, *e.g.*, "abiotic").

The significantly greater removal of DO and DOC in biotic columns indicated the presence of an active biofilm, which we presumed to be responsible for the observed microbial activity. Based on the observations, we further concluded that aerobic conditions dominated in the columns (except for anoxic niches, which may be present in biochar/porous media). Because there was no significant difference in DOC removal between "Sand, biotic" and "BC + Sand, biotic" conditions ($p = 0.27$; paired-sample t-test, $\alpha = 0.05$), we concluded that DOC removal after initial conditioning (~day 11 after column inoculation) was governed by microbial activity rather than adsorption to the biochar. These findings correspond well to another study comparing chemical oxygen demand (COD) between sand and activated carbon (AC) biofilters, concluding that the type of filter material did not affect the activity of the heterotrophic biomass and hence that biotransformation was the main mechanism responsible for COD removal.[60]

3.2. Impact of fouling/ageing on biochar properties

To comparatively assess the impact of biological fouling and ageing (over 115 days total) on biochar physical properties and thus sorption, fresh and aged (both biotic and inhibited) biochar samples collected from columns were analyzed for total pore volume (PV) and BET specific surface area (BET SSA) (Fig. 1b). The largest portion (75.4%) of the total PV of fresh MCG biochar was attributed to the mesopore fraction (pore sizes 20–500 Å or 2–50 nm), followed by micropore volume (17.0%; <20 Å or <2 nm), whereas the smallest fraction was comprised of macropores (7.6%; >500 Å or >50 nm). A high degree of mesoporosity is reportedly crucial for the sorption of triazine herbicides to biochar: mesopores were beneficial in minimizing steric hindrance effects and may provide pathways for contaminants to diffuse into deeper pores.[30] The BET SSA of fresh MCG biochar was 641 $m^2\ g^{-1}$, and is approximately double the value reported elsewhere[27] for the same type of biochar (317 $m^2\ g^{-1}$). As both biochars were acquired from the same production facility but originated from different production batches, this may explain the variability in physical properties. Interestingly, the relative reduction in BET SSA and PV over time was more pronounced under inhibited fouling conditions compared to biologically active conditions (reduction by 85% and 45%, respectively, for inhibited *vs.* 70% and 23%, respectively, for biotic), which could be indicative of a regenerative effect of microbial activity, potentially through elevated DOC consumption over time that frees up sorption sites at the biochar surface.

3.3. Column performance: contaminant breakthrough curves

The removal of the parent compounds atrazine, imidacloprid, and clothianidin followed a similar pattern in the different treatment conditions (Fig. 2): sand columns (both biotic and inhibited) broke through ($C_{Effluent} = 0.05 \times C_{Influent}$) nearly immediately (<0.71 d) for all three compounds. Breakthrough curves (BTCs) for the TOrCs indicated relatively rapid initial breakthrough in the inhibited BC + sand column as well (3.03 d, 3.14 d, and 4.45 d to initial breakthrough for clothianidin, atrazine, and imidacloprid, respectively), but in

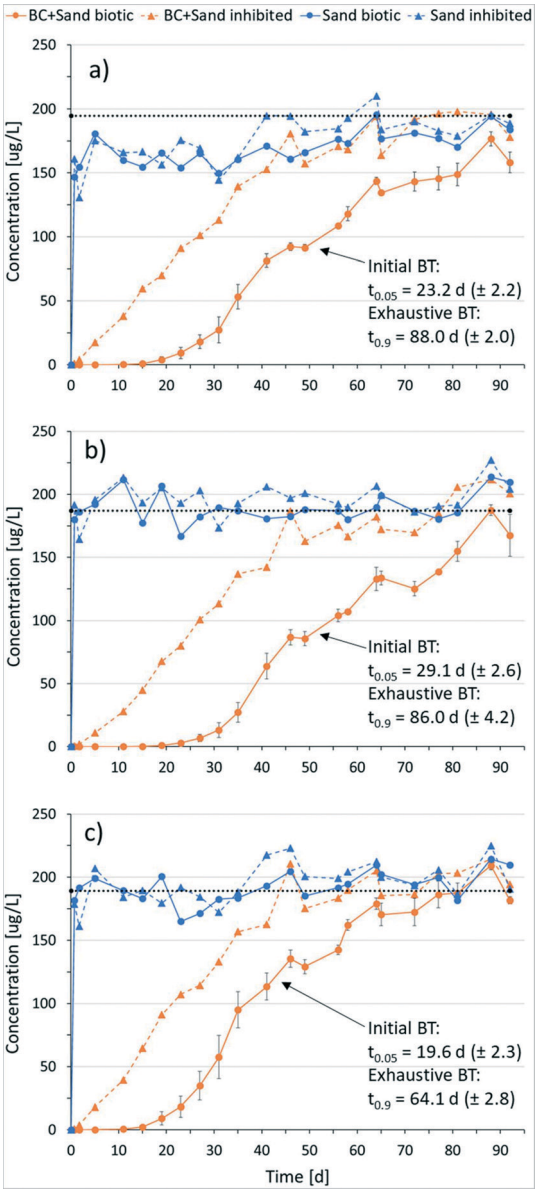

Fig. 2 Column effluent concentrations [μg L^{-1}] over time [days] for the spiked pesticides: a) atrazine, b) imidacloprid, c) clothianidin. Initial breakthrough (BT) is defined as the time when the effluent concentration C_w = 0.05 × $C_{influent}$, and exhaustive BT is defined as the time when the effluent concentration C_w = 0.9 × $C_{influent}$. BT times for the 'BC + Sand biotic' condition (three replicates) are reported as mean ± standard deviation. Dotted lines represent the mean influent concentrations.

a more gradual manner compared to the biotic treatment (linear *vs.* s-shaped BTCs). Initial breakthrough times of biotic BC + sand columns occurred in the following order: clothianidin ≤ atrazine < imidacloprid. When the batch isotherm-derived Freundlich parameters (Table S4,† discussed further below) are used to calculate K_d values at C_W = 10 μg L^{-1} (K_d = 151 000, 117 000, and 114 000 L kg^{-1} for imidacloprid, atrazine, and clothianidin, respectively), these coefficients appear to be good predictors of initial column breakthrough order in the biotic BC + sand columns, despite isotherm nonlinearity. However, the order of compounds did shift slightly when it came to average exhaustive breakthrough time (defined as the time when $C_{Effluent}$ = 0.9 × $C_{Influent}$) and was as follows: clothianidin < imidacloprid ≤ atrazine.

The enhanced performance with respect to pesticide removal in the biotic BC + sand columns is likely due to the combined presence of biochar and (active) microbial biofilm. Because sand was the dominant material in our study (from a mass perspective) and biochar was only present at 0.5 wt%, the biofilm may have been primarily located on the sand particles. Despite this, the data suggest that the biochar played a crucial role for pesticide fate and removal involving the biofilm: even though DO and DOC removal in the biotic sand columns (without biochar) were similar to those with biochar (Fig. 1), there was a major difference in pesticide removal between these two conditions (Fig. 2). There was almost no removal of pesticides in the biotic sand column (no biochar) despite comparable DOC and DO removal. In short, there is a clear difference between the fate of DOC and pesticides in these systems: this is evident from the differences in removal between the biotic and inhibited systems and it does point to a clear role of biochar in promoting pesticide removal.

3.4. Biotic contributions to overall TOrCs removal

3.4.1. Parent mass balance (columns). To study the relative importance of biodegradation in overall TOrCs removal, the cumulative mass removal for each of the conditions was calculated over the course of the experiment. Because both biotic and inhibited BC + sand systems were inoculated with a microbial biofilm, we attribute the difference in long-term TOrCs removal to microbial activity (and not simply biosorption), potentially involving biodegradation. The mass balance in Fig. 3 was developed based on area under the curve calculations of BTCs of TOrC effluent concentrations shown in Fig. 2. The difference in cumulative mass removal at specific timepoints (Fig. 3) between biotic BC + sand and inhibited BC + sand (assumption: sorption only) was assumed to yield the "biotic contribution" or biodegradation portion of the overall removal.

The contributions of both sorption and biodegradation to overall removal varied through time (Fig. 3). As can be expected based on exhaustion of sorption sites and pore filling, the share of sorption in overall mass removal decreased over time. Concurrently, the share of biodegradation increased between 30 and 60 days. We estimated biotic contributions to account for 20–36% of overall biologically enhanced removal in biotic BC-amended sand columns. These results correspond well with findings from a previous study,[61] which reported that the presence of a biofilm improved the removal of nine pharmaceuticals in a biological activated carbon filter (BAF) and that the contribution of biofilm in overall removal of these compounds was in the range of 22–35%. Indeed, Frankel *et al.*[32] reported that biochar-attached biofilms resulted in higher

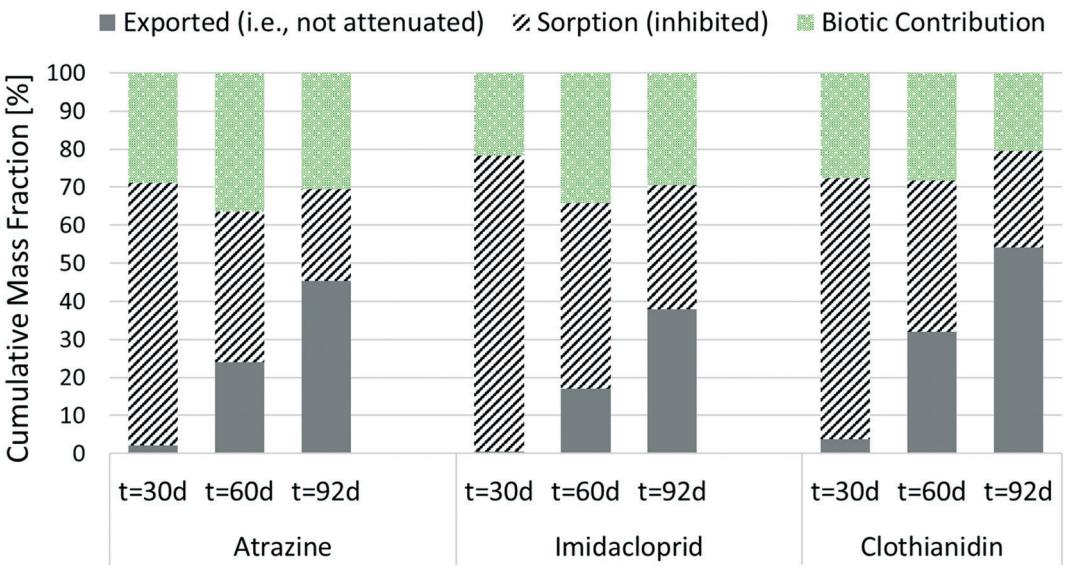

Fig. 3 Mass balance of parent effluent data (area under curve calculation). The share of sorption, inhibited (comprising both sorption to the biochar and biosorption) was estimated from the difference between the inhibited sand and inhibited BC + sand breakthrough curves. This portion was then subtracted from the biologically enhanced removal observed in the biotic BC + sand columns to yield the biotic contribution (consisting of both biologically enhanced sorption and biodegradation).

removal of naphthenic acids (42–72%) compared to sterile biochar experiments (22–25%). Nevertheless, the dominant removal mechanism may change over time, which was the case in a system simulating natural groundwater recharge when prevalence shifted from sorption to biodegradation.[46]

In the present study, our mass balance indicates that a biochar application rate of 0.5 wt% and the presence of an active biofilm prolonged the observed biofilter lifetime by 1.8–2.3 times compared to a fouled but inactive filter dominated by adsorptive removal only (inhibited BC + sand) (Fig. 3). This finding contradicts the common concept (*e.g.*, in the case of recalcitrant compounds) that biofilm growth (or biofouling) may decrease the lifetime of adsorptive biochar filtration systems.[28] A mass balance of the parent compounds, however, does not allow for any firm mechanistic conclusions: the biotic contributions may be due to a combination of biotransformation and biologically enhanced sorptive removal. The latter process may be separately studied only in the case of non-biodegradable compounds such as PFASs: a recent study investigated removal of PFASs from wastewater in laboratory column experiments and showed that the activity of the microbial biofilm appeared positively related to the enhanced sorptive removal of PFASs.[62] The authors argued that – compared to the inactive biofilm–biochar – the activity of the biofilm may have led to an increased number of available sorption sites on the biochar by continuously degrading organic matter (*i.e.*, DOC in the influent). Our findings of decreased fouling (lessened decline of SSA and PV; see section 3.2) under biologically active conditions are consistent with this hypothesis and potentially point towards biologically enhanced sorptive removal and thus a regenerative effect of microbial activity restoring some of the sorption capacity over time.

Biotransformation of organic chemicals in the combined presence of a microbial biofilm and biochar may involve several mechanisms, which may occur simultaneously and are thus not mutually exclusive. In addition to degradation in the aqueous phase, literature indicates that biodegradation of biochar-bound organic compounds may be possible due to bioregeneration[63] or enhanced desorption[48] and due to the biochar's ability to serve as redox catalyst between microorganisms and organic compounds.[42] Bioregeneration occurs during water treatment employing combined biological and adsorptive processes, in which microorganisms renew the adsorption capacity of the black carbon.[44] Traditionally, it is thought that a concentration gradient between the carbon surface and the bulk liquid is a prerequisite for bioregeneration.[44] This gradient leads to the desorption of activated carbon-bound organics and renders them available for microorganisms in the aqueous phase.[44] Abromaitis *et al.*[64] argue that the reversibility of adsorption is highly dependent on the activation energy of desorption. Because of this, mesoporous adsorbents might be more favorable for desorption and hence bioregeneration than microporous, *e.g.*, commercially available GAC.[63,64] The biochar used in our study was predominantly mesoporous (75.4% of total PV) and might thus be well suited for bioregenerative processes. Yu *et al.*[65] studied the desorption behavior of the pesticide diuron in soil and the role of biochar microporosity and found a high correlation between adsorption–desorption hysteresis and micropore volume. Assuming that bioregeneration is dependent on a concentration gradient, activated carbon regeneration may only be induced after major changes in the loading or operation of the treatment system, *e.g.*, wash-out in a BAC system, which lowers the bulk concentration.[64] We posit that from this perspective, variable influent systems such as stormwater

treatment structures may create conditions favorable for bioregeneration. For example, some catchments may exhibit a first flush phenomenon for certain contaminants, meaning that highly concentrated water is followed by cleaner stormwater runoff.[66,67] In other cases, however, stormwater pollutographs may be more complex than the simple first flush concept,[68] or pollutant concentrations may be subject to seasonal variability.[69]

Microbial degradation processes of biochar-sorbed organic chemicals are different compared to organics present in the dissolved phase and DOC may substantially impact their desorption and mineralization rates. Zhang *et al.*[48] demonstrated that the presence of humic acid (HA) increased the mineralization rate of biochar-bound phenanthrene by accelerating its desorption rate into the aqueous phase. Desorption was negatively correlated with the microporosity of biochars: the authors argued that organics bound to the intraparticle surfaces and micropores may be inaccessible.[48] In our study, it is possible that a continuous source of DOC in the presence of a predominantly mesoporous biochar led to increased desorption rates and facilitated transport of atrazine, imidacloprid, and clothianidin in our biologically active columns.

Further, biochar may be crucial in facilitating reduction/oxidation reactions with organic chemicals.[40] In the presence of biochar, several coexisting degradation pathways were proposed to contribute to the biological reduction of pentachlorophenol (PCP): 41% of the PCP loss was attributed to electrical conductor mediated reduction of adsorbed PCP.[42] Unlike the mechanisms described for bioregeneration or DOC-enhanced desorption, this process is thought to act directly on the biochar-bound organics. Similarly, an alternative explanation for observed bioregeneration invokes the release of microbial exoenzymes, which react with the carbon-bound substrates/compounds,[44] thus increasing the bioaccessibility of the compounds.[70] This process may be comparable to plant root exudates stimulating the degradation of organic compounds by rhizosphere-associated microbes.[53,71] Though it remains uncertain whether and to what extent these alternative mechanisms are responsible for the enhanced removal of clothianidin, atrazine, and imidacloprid in the biochar-amended columns studied here, it is clear that the biologically active systems had a greater capacity for removal of these contaminants than the inhibited systems. The observed enhanced removal may possibly involve a combination of several coexisting processes (*i.e.*, degradation in the aqueous phase, bioregeneration, DOC-enhanced desorption and transport, biochar-bound microbial degradation).

3.4.2. Known transformation products and pathways. TP analysis offers another line of evidence to probe answers about biological processes occurring in the biofiltration columns. We detected multiple TPs of atrazine and imidacloprid in column effluents at timepoints during column operation (Fig. 4): desethyl-atrazine (DEA), 2-hydroxy-atrazine (OH-ATZ), desnitro-imidacloprid (desnitro-IMI), and imidacloprid–olefin (IMI–olefin). Concentrations were generally highest in biotic BC + sand systems and of greater

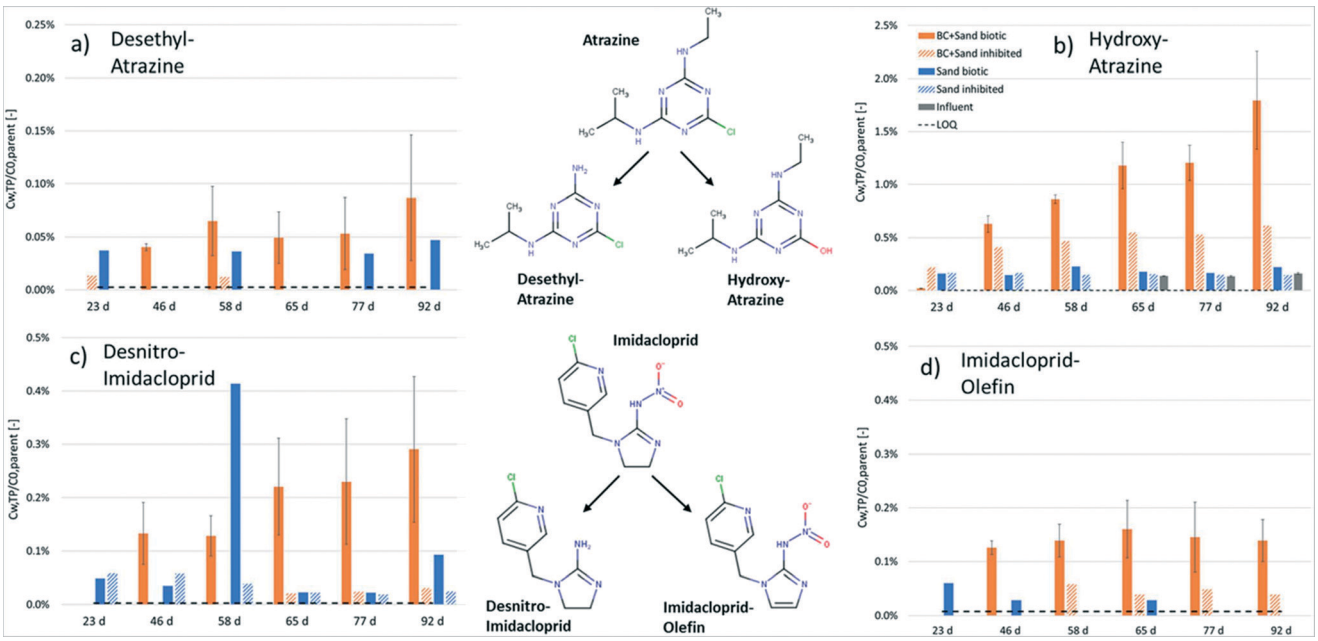

Fig. 4 Temporal evolution of transformation products (TPs) of atrazine and imidacloprid in column effluents and influent identified by target LC-QToF-MS analysis: a) desethyl-atrazine, b) 2-hydroxy-atrazine, c) desnitro-imidacloprid, d) imidacloprid–olefin. *Y*-Axis shows TP concentrations in effluent normalized by the average parent influent concentration (Cw, TP/C0, parent). Dotted black lines represent the limit of quantitation (LOQ) for each TP.

consistency compared to control conditions (Fig. 4), although fractions of TPs normalized to parent influent concentrations remained below 2.5% for all conditions throughout the entire experiment. This indicates that biodegradation was occurring, but quantitative estimations are complicated by a lack of authentic standards, yet unknown TPs, as well as the uncertainty as to the degree of mineralization *vs.* transformation. Interestingly, in the early stage of the experiment (at t = 23 d), TPs were primarily detected in biotic sand columns, but not yet in biotic BC + sand systems (with the exception of OH-ATZ). Suspect TP peaks were also found for deisopropylhydroxy-atrazine and didealkylatrazine, with both offering some MS2 data to provide more confidence in their detection (*i.e.*, some had library scores >90); however, the peaks were deemed to be false positives caused by in-source fragmentation of OH-ATZ and DEA, respectively, based on their respective retention times and their presence in analytical standards containing OH-ATZ and DEA (Fig. S14 and S15†).

Among all the TPs examined, the highest production was found for OH-ATZ. Levels of OH-ATZ in the effluent of the biotic BC + sand columns exhibited a clear increasing trend over time (R^2 = 0.98, linear regression). Differences in concentrations between the four tested conditions in the time range 46–92 days were only statistically significant between biotic BC + sand and each of the biotic and inhibited sand controls (p = 0.0423 and p = 0.0036, respectively; Dunn's multiple comparisons test). Detections of OH-ATZ in both biotic and inhibited sand controls were in the range of levels observed in the influent, which were most likely attributable to aqueous hydrolysis governed by solution pH.[72] OH-ATZ in inhibited BC + sand columns was likely produced *via* surface-catalyzed hydrolysis induced by the biochar, a process that has been described for atrazine.[72] Possible mechanisms behind the biochar-enhanced hydrolysis of atrazine include surface-bound metal atoms facilitating the nucleophilic attack of water molecules and surface hydroxyl groups acting as nucleophiles. Biochar-catalyzed reductive transformation was also reported for the dinitro herbicides pendimethalin and trifluralin *via* similar mechanisms.[73] Production of DEA in the columns is likely related to the presence of the microbial biofilm, as DEA was almost exclusively observed in the biotic BC + sand columns, although also (inconsistently) in biotic sand columns. Over the entire course of the experiment, concentrations of DEA were lower compared to OH-ATZ (in biotic BC + sand columns: p = 0.0048; paired-sample t-test, α = 0.05), consistent with observations in soil and aquatic systems, where the hydroxylation pathway is generally more common for atrazine.[74] From an environmental risk perspective, hydroxylation renders OH-ATZ non-herbicidal (unlike DEA and DIA) and thus is considered a more straightforward detoxification pathway.[75,76]

The prevailing redox conditions may have a strong impact on atrazine degradation, and generally, degradation rates are faster under aerobic compared to anaerobic conditions. For example, Douglass *et al.*[77] studied the mineralization of atrazine in wetland sediments and the aerobic half-life of atrazine was roughly a week, whereas half-lives under anaerobic conditions were up to 50 days. In the present study, the DO levels in effluents of biotic columns were 3.84 ± 0.91 mg L^{-1} (BC + sand) and 4.03 ± 1.05 mg L^{-1} (sand), indicating predominantly aerobic conditions, except for potential anoxic/anaerobic microniches present in the porous media.

Among imidacloprid TPs, concentrations of desnitro-IMI were highest in biotic BC + sand columns (except for t = 58 d) and followed a clear temporal trend (R^2 = 0.88, linear regression; Fig. 4). Desnitro-IMI was detected in effluents of all control columns, but at variable levels. The presence of desnitro-IMI in inhibited sand columns suggests that either abiotic degradation occurred (although, hydrolysis of imidacloprid under environmentally relevant conditions is very unlikely)[78] or that sufficient biological activity in the inhibited columns transformed imidacloprid to desnitro-IMI. Similarly, concentrations of IMI–olefin were highest in biotic BC + sand columns, but IMI–olefin was also present (to a lower extent) in biotic sand and inhibited BC + sand systems. 5-Hydroxy-imidacloprid (5-OH-IMI) and nitrosoguanidine-imidacloprid (NG-IMI) were detected *via* suspect screening of column effluent samples. Precursor peaks for both NG-IMI and 5-OH-IMI were consistently detected in biotic BC + sand samples over time, but only NG-IMI could consistently be confirmed by one accurate mass fragment (209.0591 Da; for details see Table S6†). We presume that 5-OH-IMI precursor peaks were too small for consistent fragment accurate mass confirmation. This led to the assignment of different suspect confidence levels according to the Schymanski scale:[54] level 3 for NG-IMI and level 4 for 5-OH-IMI (Table S6†).

Typically, biotransformation is associated with detoxification mechanisms that render metabolites less toxic than their parent compound. However, for some 'target-specific' pesticides such as imidacloprid and other neonicotinoids (*i.e.*, pesticides that are designed to impart toxicity to certain pests *via* enhanced receptor binding specificity), decreased toxicity does not necessarily occur with degradation. Specifically, insect selectivity (*i.e.*, differential binding propensity toward insect receptors) and thus the toxicity of neonicotinoids is due to favorably binding to the insect nicotinic acetylcholine receptor (nAChR) and is effectively repelled by vertebrate nAChRs (including mammalian).[79] Replacing the $=NNO_2$ group in imidacloprid by =NH to yield desnitro-IMI inverts the selectivity for insect *versus* mammalian receptors, rendering desnitro-IMI >300 times more toxic (based on binding affinity data) toward mammals while at the same time greatly decreasing its insect toxicity.[79] In contrast, the acute toxicity of IMI–olefin towards insects is even higher than imidacloprid, as highlighted in exposure studies on cotton whiteflies[80] and honey bees.[81] IMI–olefin and desnitro-IMI are part of two distinct transformation pathways of imidacloprid: IMI–olefin is considered a "dead-end product", whereas the latter is an

intermediate product in the pathway that may lead to complete mineralization *via* IMI-urea (Fig. S2†). Therefore, despite the increased mammalian toxicity, degradation into desnitro-IMI might still be preferred from an environmental risk perspective, because it may further transform into TPs that are, during acute exposure, reportedly less insecticidal (lower bee mortality) compared to imidacloprid.[81]

6-Chloronicotinic-acid (6-CNA) is a TP of imidacloprid and other neonicotinoids, *e.g.*, acetamiprid,[82] and is to be found at the "lower end" of the microbial degradation pathway of imidacloprid (Fig. S2†). In some bacterial biodegradation studies, 6-CNA was reported as a dead-end metabolite, whereas most evidence indicates full mineralization is possible.[83] In the present study, 6-CNA was detected at low concentrations in effluents of biotic BC + sand columns towards the end of the column experiment. At 92 days after the onset of spiking, 6-CNA was measured at 0.091 μg L^{-1} in one column replicate and detected below the LOQ of 0.05 μg L^{-1} in another replicate. The relatively low concentrations of 6-CNA observed argues against it being a dead-end metabolite. As for the other experimental conditions, 6-CNA was neither detected in any of the inhibited column controls (sand or BC + sand, respectively) nor in the influent water. Although 6-CNA causes considerably less bee mortality than the parent imidacloprid,[81] it may still induce some oxidative stress towards aquatic non-target organisms such as freshwater algae and crustacean amphipods.[84] Moreover, the chronic toxicity towards bees was found to be equally high for imidacloprid and its major TPs, including 6-CNA.[81]

At the time of the analysis, there were no analytical standards or entries in spectral libraries available for the identification of clothianidin TPs. Employing a suspect screening approach (Table S3†), we confirmed the presence of one potential TP in effluents of biotic BC + sand columns, namely clothianidin-urea (CLO-urea) with a protonated precursor accurate mass of 206.01494 Da. All reported peaks fulfilled the suspect precursor quality criteria (<5 ppm mass error, <40% difference in isotope ratio) and the peak identity was further confirmed *via* at least one known unique fragment ion accurate mass (<10 ppm fragment mass error). The peak area counts in select column effluent samples were converted into concentration values using a semi-quantitation approach with clothianidin as the calibrant (calculations see ESI†). The resulting concentrations of CLO-urea were in the range of 1 μg L^{-1} and were highest at the end of the experiment (t = 92 days) (Fig. S13c†). Thus, CLO-urea levels were likely in the same order of magnitude as other target TPs and were only surpassed by OH-ATZ concentrations.

N-(2-Chlorothiazol-5-yl-methyl)-*N*′-nitroguanidine (TZNG) and *N*-methyl-*N*′-nitroguanidine (MNG) are among the most common biodegradation TPs of clothianidin, based on results of soil degradation studies under dark aerobic conditions at 20 °C (Fig. S3†).[85] Mori *et al.*[86] conducted a degradation study of clothianidin under nitrogen-limited conditions using a specific microorganism, the white-rot fungus *P. sordida*, which is known to produce enzymes that catalyze the degradation of recalcitrant organic chemicals. The fungus degraded 37% of clothianidin in 20 days and CLO-urea (or *N*-(2-chlorothiazol-5-yl-methyl)-*N*′-methylurea; TZMU) was the main observed metabolite.[86] A study investigating the biodegradation of clothianidin in agricultural soils from China identified CLO-urea and a second compound (m/z = 170.9; potentially dechlorinated form of CLO-urea) as degradation products.[87] In contrast to atrazine and imidacloprid, clothianidin undergoes faster biodegradation under anaerobic compared to aerobic conditions, with degradation rates also dependent on factors such as temperature, nutrient levels, and initial concentration.[88] CLO-urea has also been reported as a hydrolysis product of clothianidin (at ≥50 °C and pH 9);[85] however, at ambient temperatures, clothianidin is considered hydrolytically stable in the pH range of 4–9.[85,89] In short, while there are limited clothianidin biodegradation data available, CLO-urea was one of the metabolites that was commonly reported in other degradation studies. The prevailing environmental conditions in our study (aerobic except for micro niches, T = 20 °C) may not have been optimal for clothianidin degradation. From a toxicity standpoint, it appears that CLO-urea may be less toxic than its parent compound, as clothianidin significantly decreased the viability of neuroblastoma cells, while CLO-urea did not show significant effects (up to 300 μM):[86] transformation of clothianidin to CLO-urea would likely be a desired goal of a biofilter. Our combined suspect screening and semi-quantitation approach revealed that CLO-urea was indeed an important TP of clothianidin and should be considered in future studies.

Overall, our findings suggest that biodegradation is predominantly occurring in both the "traditional" (sand biotic) and the biochar-amended biofilters (BC + sand biotic), however, only the latter offers the crucial benefit of contaminant retention that ultimately leads to treatment of the stormwater.

3.4.3. Microcosm mass balance/suspect screening. We conducted microcosm experiments to study the transformation of atrazine, imidacloprid and clothianidin under non-sorptive conditions (no biochar) and using the same microbial enrichment solution that was used for column inoculation. The goal was to determine if differences in TPs between microcosms and column effluents could be attributed to the presence of biochar. Initial concentrations in the microcosms (415 μg L^{-1}, 361 μg L^{-1}, and 364 μg L^{-1} for atrazine, imidacloprid, and clothianidin, respectively) were higher than in column influents to increase the opportunity for detecting TPs produced at very low levels. After 369 days, overall parent mass removal in the two biotic microcosm replicates were 15.0% (±4.73), 34.1% (±0.01), and 18.8% (±0.08) for atrazine, imidacloprid, and clothianidin, respectively. In a biotransformation experiment using biofilms collected from natural streams, Desiante *et al.*[90] considered imidacloprid recalcitrant since concentration

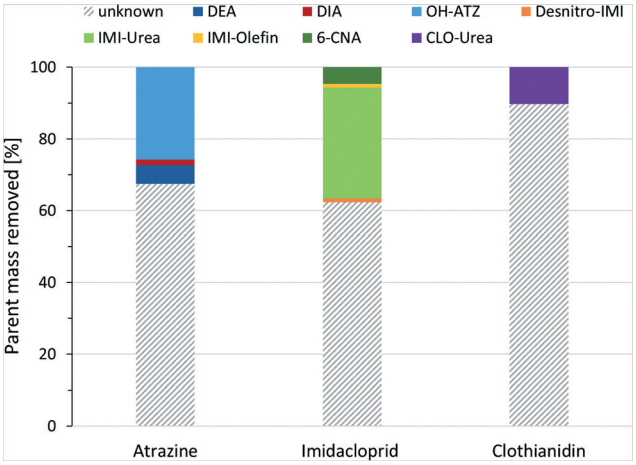

Fig. 5 Molar mass balance of microcosm data: share of transformation products in total parent mass removal at the end of the experiment (369 days). The total parent molar masses removed after 369 days were 71.4 nmol, 119.2 nmol, and 67.8 nmol for atrazine, imidacloprid, and clothianidin, respectively. Initial concentrations for the three compounds were 1923 nM, 1412 nM, and 1458 nM, respectively. "Unknown" indicates that the mass was unaccounted for. Abbreviations: desethyl-atrazine (DEA), desisopropyl-atrazine (DIA), and 2-hydroxy-atrazine (OH-ATZ), desnitro-imidacloprid (desnitro-IMI), imidacloprid-urea (IMI-urea), imidacloprid–olefin (IMI–olefin), 6-chloronicotinic acid (6-CNA), and clothianidin-urea (CLO-urea). Note that calculations for CLO-urea are semi-quantitative.

decreases of <20% were observed over the course of 72 hours. Imidacloprid was also classified persistent according to REACH and EMA guidelines in lake/river sediment suspension experiments.[91] For atrazine, however, average removal of 45% was observed in biotic microcosms over the duration of 76 days.[33]

All seven target TPs that were detected in column effluents were present in the microcosm solutions as well (Fig. 5; Table S7†). The most abundant TP of atrazine was OH-ATZ, while for imidacloprid, the highest concentrations were detected for IMI-urea, followed by 6-CNA. Similarly, Muerdter and LeFevre[53] recently found IMI-urea and 6-CNA – which are both less potent insecticides compared to their parent[81,84] – as the main degradation products of imidacloprid in a synergistic duckweed-microbial system. Again, when it comes to chronic insect toxicity, however, there may be no difference between imidacloprid and its major TPs.[81]

Suspect screening of microcosm samples revealed the presence of the same TPs that were also found in biotic column samples: 5-OH-IMI, NG-IMI, and CLO-urea. Precursor peaks for all three suspects were consistently detected in microcosm samples over time, but only CLO-urea could be confirmed by one accurate mass fragment at the end of the experiment (369 days). 5-OH-IMI precursor peaks were too small for consistent fragment accurate mass confirmation, and NG-IMI peaked during earlier stages of the experiment and peaks were too low to be confirmed at the end (Fig. S12†). Suspect concentrations were estimated employing a semi-quantitation approach using calibrants that share similar ionizable functional groups (details see ESI†). Suspect precursor and fragment masses, as well as representative MS and MS/MS scans for each suspect can be found in the ESI† (Table S6 and Fig. S9–S11).

Our results indicate that the target and suspect products only account for <40% of total parent mass removed (after 369 days; Fig. 5). Without authentic standards for the suspect compounds or tracking of radio-labelled parent compounds, it is unclear to what extent errors in estimated concentrations would account for the missing mass. Hence, even without the presence of biochar, potentially unknown TPs for all three pesticides makes closing the mass balance difficult. As all TPs reported here are likely semi-stable intermediates, we recognize that TP production and further degradation (*i.e.*, mineralization) may be dynamic and not well captured in a simple mass balance approach like the one employed here. Nevertheless, biodegradation was active in the microcosms, and the observed TPs were the same as in biotic column systems (both sand and BC + sand).

3.5. Abiotic batch sorption experiments

Both Freundlich and Langmuir sorption equations were fit to the batch isotherm data up to equilibrium solution concentrations of 45 μg L^{-1} (Fig. S4†). Akaike's information criterion (AIC) was used to compare the goodness-of-fit for both sorption equations, and demonstrated better fits for the Freundlich isotherm for all three parent compounds. The corresponding AIC and best-fit values of the non-linear Freundlich isotherm coefficient K_F (sorption affinity) and the Freundlich isotherm exponent n are reported in the ESI† (Table S4). The Freundlich isotherm has been used in previous studies to describe sorption of hydrophilic TOrCs to MCG-biochar[47] and of neonicotinoids to pig manure and maize straw-derived biochars.[92]

Atrazine is a weak base (pK_a = 1.6) and exists in its neutral form at environmentally relevant pH values.[93] Besides hydrophobic effects, π–π electron–donor acceptor (EDA) interactions are relevant for atrazine sorption to biochar, due to the electron donor nature of atrazine's ring substituents.[30] Imidacloprid and clothianidin are not charged at circumneutral pH (ref. 94) but have a charge distribution at their nitro group ($-NO_2$) and thus exhibit a distinct pharmacophore (see Fig. S2 and S3†). Zhang *et al.*[92] investigated the biochar sorption mechanisms of imidacloprid and clothianidin and concluded that at higher production temperatures (>500 °C), hydrophobic partitioning became less important, and instead specific interactions such as π–π EDA complexes were more prominent. Similarly, Webb *et al.*[95] suggested that imidacloprid (and imidacloprid urea) sorption may be primarily driven by π–π or π^+–π interactions (in contrast to desnitro-imidacloprid). $\log K_{OC}/\log K_{OW}$ ratios can be used as a semi-quantitative approach to assess the importance of hydrophobic effects in overall sorption and higher ratios generally indicate greater importance of specific interactions.[96] At C_W = 50 μg L^{-1} and using the K_d values

from section 3.3 for K_{OC}, we observed larger $\log K_{OC}/\log K_{OW}$ ratios for imidacloprid (9.26) compared to clothianidin (7.85), which were in line with results for de-ashed maize straw biochars produced at 700 °C.[92] Greater ratios may indicate that polar specific interactions were more important for imidacloprid sorption compared to clothianidin.[92] For atrazine, we calculated a $\log K_{OC}/\log K_{OW}$ ratio of 1.83, which indicates a higher importance of hydrophobic interactions compared to the two neonicotinoids.

Kinetic sorption data were used to compare the biochar sorption affinity at equilibrium ($K_{d,Eq} = C_{S,Eq}/C_{W,Eq}$; see Table S5; Fig. S5†) between parent compounds and TPs at an environmentally relevant initial concentration of 10 μg L^{-1}. The equilibrium K_d values of all TPs were lower compared to their respective parent compounds, which is in line with the observation that TPs are generally more polar than their parents and thus potentially more mobile in the environment.[21,97] In the case of atrazine TPs, the difference in $K_{d,Eq}$ values compared to atrazine was statistically significant in the cases of DEA and DIA ($p < 0.001$ for both) but not OH-ATZ ($p = 5.47 \times 10^{-2}$). Among imidacloprid TPs, only IMI-urea exhibited a significantly different equilibrium K_d compared to the parent compound ($p < 0.001$). Moreover, the differences in sorption affinity between the three parent compounds were not statistically significant (see Table S5†), even though the octanol–water partition coefficient of atrazine is different by two orders of magnitude from the two neonicotinoids ($\log K_{OW}$ = 2.82, 0.56, and 0.64‡ for atrazine, imidacloprid, and clothianidin, respectively). Interestingly, the loss of the electronegative pharmacophore (nitro group) during the transformation of imidacloprid to desnitro-IMI changes the metabolite's pharmacophore charge distribution to positive (amine group), which was demonstrated to have significant effects on sorption to black carbon primarily due to electrostatic interactions.[95,98] However, alteration of the pharmacophore did not explain our findings regarding imidacloprid and desnitro-IMI: for MCG-biochar, the equilibrium sorption capacities ($K_{d,Eq}$) were similar for the parent compound and the TP. Though an assessment of the surface functionalization of the biochar employed here was beyond the scope of the study, prior research indicates that sorption of desnitro-IMI is greatly impacted by surface functionalization.[95]

3.6. Transport modelling

3.6.1. Parameter estimation (fitting). Preliminary results of the modelling of atrazine, imidacloprid, and clothianidin BTCs in MATLAB revealed that sorption parameters derived from abiotic batch data were poor estimators of column performance for both the inhibited and biotic BC + sand conditions (see Fig. S16 and S17†). As the batch data set was a strong predictor of the sorption *capacity* in the inhibited BC + sand case (great agreement of linear distribution coefficients K_d at C_W = 50 μg L^{-1}; Table S10†), we attribute the difficulties in BTC prediction mainly to kinetics. Furthermore, it should be noted that tortuosity (τ) in this transport model should be regarded as a kinetic fitting parameter rather than a physically meaningful parameter (observed tortuosity values are typically below 3). The inaccuracies of the tortuosity values are likely caused by inaccuracies of other model parameters, *i.e.* diffusion coefficients. For example, as was shown for PFASs, the fitted tortuosity values might be in error due to inaccurate estimations of diffusion coefficients.[99] Hence, forward prediction of effluent BTCs based on batch data was not possible for conditions with a biofilm present (active or inactivated), unlike what was demonstrated for abiotic biochar–sand columns previously.[27] Similarly, Liu *et al.*[59] showed that GAC batch study distribution coefficients (K_d) for PFASs were not representative of model K_d values obtained from the GAC pilot-scale study.

In the present study, all model parameters were directly derived from the observed column data. We estimated the sorption to the non-BC materials using the inhibited sand column data set and these parameters (K_S, k_S; reported in the ESI†) were subsequently used to derive the sorption to the BC in the other columns. Freundlich model sorption parameters used in the subsequent scenario modelling (Table 1) were estimated based on best-fit simulations of biotic BC + sand breakthrough curves for atrazine, imidacloprid, and clothianidin (Fig. S19†). Though the intended use of this model fitting of the observed column data was primarily for estimating filter lifetimes (*i.e.*, scenario modeling), fitting of the breakthrough data revealed that the model assuming sorption-retarded intraparticle diffusion provided a better description of the data than the model assuming instantaneous sorption equilibrium. Best-fit values for the Freundlich isotherm coefficient, $K_{Fr,BC}$, were 1519, 1499, and 892 (μg g^{-1}) (L $\mu g^{-1})^n$ for atrazine, imidacloprid, and clothianidin, respectively.

In the column model used in this study, biodegradation can be accounted for through the parameter k_{deg}, which is the first-order biodegradation rate for the pollutant in the mobile water (see ESI† for more information). The model assumes that a biodegradation rate of $k_{deg} > 0$ will lead to a reduction of the maximum possible breakthrough concentration ($C_w/C_0 < 1$) at steady state. However, in our case, these assumptions may not hold: 1) pesticide breakthrough in the biotic BC + sand columns was dynamic and not at steady state, and; 2) the mass removal rate of biodegradation was likely sufficiently smaller than the mass loading rate at full breakthrough. In light of the evidence discussed above, various biological and synergistic processes may have contributed to the removal of the pesticides in the biologically active columns. Biodegradation was likely more complex in the present study and may not be appropriately represented by a first-order degradation rate acting only on

‡ KOWWIN v1.68 estimates.

Table 1 Biofilter lifetime simulations based on different case study scenarios. Bold numbers indicate biofilter lifetime estimates when treating 16 inches of annual rainfall (Denver, CO), and numbers in parentheses represent biofilter lifetimes assuming continuous flow/operation. Freundlich parameters represent best-fit values to biotic BC + sand column data, assuming kinetic diffusion limitations

	Atrazine	Imidacloprid	Clothianidin
Freundlich model parameters:			
$K_{Fr,BC}$ [(μg g^{-1})(L μg^{-1})^n]	1519	1499	892
$n = 1/n_{Fr,BC}$ [—]	0.402	0.417	0.457
Tortuosity [—]	25.1	17.8	19.9
Aquatic life threshold value			
C_{Th} [μg L^{-1}]	0.60[a]	0.01[b]	0.05[b]
Scenario 1:			
M_{BC} [wt%]	1.0 (~5 vol%)		
A: Stormwater – C_{In} [μg L^{-1}]	0.624[c]	0.428[c]	0.666[d]
Time to reach C_{Th} [years]	**112 (11.8)**	**68.5 (7.2)**	**32.3 (3.4)**
B: Stream – C_{In} [μg L^{-1}]	5.17[e]	0.1428[e]	0.0663[e]
Time to reach C_{Th} [years]	**17.5 (1.8)**	**141 (14.9)**	**390 (41.1)**
Scenario 2:			
M_{BC} [wt%]	4.0 (~20 vol%)		
A: Stormwater – C_{In} [μg L^{-1}]	0.624	0.428	0.666
Time to reach C_{Th} [years]	**377 (39.7)**	**343 (36.2)**	**158 (16.7)**
B: Stream – C_{In} [μg L^{-1}]	5.17	0.1428	0.0663
Time to reach C_{Th} [years]	**83.2 (8.8)**	**672 (70.9)**	**779 (82.2)**
Scenario 3:			
M_{BC} [wt%]	6.5 (~32 vol%)		
A: Stormwater – C_{In} [μg L^{-1}]	0.624	0.428	0.666
Time to reach C_{Th} [years]	**593 (62.6)**	**579 (61.1)**	**266 (28)**
B: Stream – C_{In} [μg L^{-1}]	5.17	0.1428	0.0663
Time to reach C_{Th} [years]	**139 (14.7)**	**1120 (119)**	**1300 (137)**

[a] Environmental quality standard (EQS) value, annual average for surface waters (European Union). [b] Chronic aquatic life benchmark for invertebrates, for freshwater (U.S. EPA). [c] Spahr *et al.* 2020.[11] [d] Sutton *et al.* 2019.[100] [e] Bradley *et al.* 2017.[101] Abbreviations: M_{BC} = biochar application rate, C_{In} = influent concentration.

dissolved phase contaminants (as biodegradation could also happen in the sorbed phase). Therefore, we did not explicitly quantify the rate of biodegradation in this model and decided to assume that for our modelling purposes, the observed mass removal difference between biotic and inhibited BC + sand columns was due to biologically enhanced sorption only (in order to be conservative and not overestimate the contribution of biodegradation in the subsequent scenario modelling). Thus, the removal due to regenerated sorption capacity over time (biologically enhanced sorption) was lumped into the sorption parameters of the Freundlich isotherm equation during the fitting process. This was reflected in 2.5–3.6 times greater values for the linear distribution coefficients K_d (derived at C_W = 10 μg L^{-1} using the fitted Freundlich sorption parameters; see Table S10†) in the biotic BC + sand condition (Fig. S19†) compared to the inhibited biochar control (Fig. S18†).

3.6.2. Biofilter lifetime simulations (scenarios). Table 1 lists simulation results from scenarios 1–3, which describe how long a biologically active biochar-amended biofilter could run in a representative field-scale scenario (Table S11†) for a residential area in Denver, CO, until it reached a defined aquatic life threshold value, C_{Th}. As expected, filter lifetimes increased with increasing biochar application rate (M_{BC}) for all three pesticides, and lifetimes were highly dependent on the respective aquatic life threshold values and influent concentrations. The shortest breakthrough times were observed for atrazine with 17.5 years (scenario 1, stream water), followed by clothianidin with 32.3 years (scenario 1, stormwater) and imidacloprid with 68.5 years (scenario 1, stormwater). Our simulations indicate that even in a worst-case scenario with 5 vol% biochar only, the biofilter could effectively remove these pesticides from an impacted water for at least 17 years without endangering aquatic life in receiving waters.

3.7. Environmental implications

Biochar amendments of biofiltration systems offer a promising solution to mitigate the environmental and ecotoxicological impacts of hydrophilic TOrCs such as herbicides and insecticides. The distributed implementation of these green infrastructure systems in an urban watershed can decrease stormwater runoff peak flows, while at the same time decreasing concentration peaks *via* enhanced contaminant removal. The latter has been shown in a watershed-scale model for the insecticide fipronil[10] and may help to protect the aquatic and human health of local surface and groundwater bodies. In this study, we demonstrated the benefit of the combined presence of biochar and biofilm in a biofilter, which promoted conditions favorable for biodegradation, enhanced-sorptive removal, and possibly a

regenerative effect to restore some of the biochar's sorption capacity over time. Our findings provide insight into the design of biofilter systems in practice: the addition of biochar in conjunction with a relatively porous media such as sand may help to establish an active microbial community in the biofilter with an estimated filter lifetime of over 15 years. A self-restoring system would certainly lead to less maintenance efforts and costs over the filter's lifetime. In practice, the presence of biofilms would most likely not be a design choice but instead an inevitable feature of biofilters due to the presence of DOC and microorganisms in stormwater and various surfaces supporting microbial attachment. Furthermore, the results of our study indicate that biochar-amended biofilters are not a significant source of TPs into the environment. More importantly, most of the TPs that were detected are less toxic than their respective parent compounds, which has important environmental risk implications. Biofilters are relatively non-invasive and, especially when vegetated, add important green space to urban areas, which may offer co-benefits beyond flood control and water quality enhancement.[102,103]

Conflicts of interest

The authors declare no competing conflicts of interest.

Acknowledgements

Support for this work was provided in part by the U.S. National Science Foundation Engineering Research Center for Reinventing the Nation's Urban Water Infrastructure (ReNUWIt) (Award No. EEC1028968). GHL was supported by NSF Grant No. 1844720.

References

1 R. G. Luthy, S. Sharvelle and P. Dillon, Urban Stormwater to Enhance Water Supply, *Environ. Sci. Technol.*, 2019, **53**, 5534–5542.
2 S. K. Mohanty, R. Valenca, A. W. Berger, I. K. M. Yu, X. Xiong, T. M. Saunders and D. C. W. Tsang, Plenty of room for carbon on the ground: Potential applications of biochar for stormwater treatment, *Sci. Total Environ.*, 2018, **625**, 1644–1658.
3 S. E. Clark and R. Pitt, Targeting treatment technologies to address specific stormwater pollutants and numeric discharge limits, *Water Res.*, 2012, **46**, 6715–6730.
4 J. E. Grebel, S. K. Mohanty, A. A. Torkelson, A. B. Boehm, C. P. Higgins, R. M. Maxwell, K. L. Nelson and D. L. Sedlak, Engineered Infiltration Systems for Urban Stormwater Reclamation, *Environ. Eng. Sci.*, 2013, **30**, 437–454.
5 G. H. LeFevre, K. H. Paus, P. Natarajan, J. S. Gulliver, P. J. Novak and R. M. Hozalski, Review of dissolved pollutants in urban storm water and their removal and fate in bioretention cells, *J. Environ. Eng.*, 2015, **141**, 04014050.
6 J. Gasperi, C. Sebastian, V. Ruban, M. Delamain, S. Percot, L. Wiest, C. Mirande, E. Caupos, D. Demare, M. D. K. Kessoo, M. Saad, J. J. Schwartz, P. Dubois, C. Fratta, H. Wolff, R. Moilleron, G. Chebbo, C. Cren, M. Millet, S. Barraud and M. C. Gromaire, Micropollutants in urban stormwater: occurrence, concentrations, and atmospheric contributions for a wide range of contaminants in three French catchments, *Environ. Sci. Pollut. Res.*, 2014, **21**, 5267–5281.
7 A. Burant, W. Selbig, E. T. Furlong and C. P. Higgins, Trace organic contaminants in urban runoff: Associations with urban land-use, *Environ. Pollut.*, 2018, **242**, 2068–2077.
8 W. W. Stone, R. J. Gilliom and K. R. Ryberg, Pesticides in U. S. Streams and Rivers: Occurrence and Trends during 1992–2011, *Environ. Sci. Technol.*, 2014, **48**, 11025–11030.
9 M. A. Rippy, A. Deletic, J. Black, R. Aryal, J.-L. Lampard, J. Y.-M. Tang, D. McCarthy, P. Kolotelo, J. Sidhu and W. Gernjak, Pesticide occurrence and spatio-temporal variability in urban run-off across Australia, *Water Res.*, 2017, **115**, 245–255.
10 J. M. Wolfand, C. Seller, C. D. Bell, Y.-M. Cho, K. Oetjen, T. S. Hogue and R. G. Luthy, Occurrence of Urban-Use Pesticides and Management with Enhanced Stormwater Control Measures at the Watershed Scale, *Environ. Sci. Technol.*, 2019, **53**, 3634–3644.
11 S. Spahr, M. Teixidó, D. L. Sedlak and R. G. Luthy, Hydrophilic trace organic contaminants in urban stormwater: occurrence, toxicological relevance, and the need to enhance green stormwater infrastructure, *Environ. Sci.: Water Res. Technol.*, 2020, **6**, 15–44.
12 K. T. Peter, Z. Tian, C. Wu, P. Lin, S. White, B. Du, J. K. McIntyre, N. L. Scholz and E. P. Kolodziej, Using High-Resolution Mass Spectrometry to Identify Organic Contaminants Linked to Urban Stormwater Mortality Syndrome in Coho Salmon, *Environ. Sci. Technol.*, 2018, **52**, 10317–10327.
13 J. R. Masoner, D. W. Kolpin, I. M. Cozzarelli, L. B. Barber, D. S. Burden, W. T. Foreman, K. J. Forshay, E. T. Furlong, J. F. Groves, M. L. Hladik, M. E. Hopton, J. B. Jaeschke, S. H. Keefe, D. P. Krabbenhoft, R. Lowrance, K. M. Romanok, D. L. Rus, W. R. Selbig, B. H. Williams and P. M. Bradley, Urban Stormwater: An Overlooked Pathway of Extensive Mixed Contaminants to Surface and Groundwaters in the United States, *Environ. Sci. Technol.*, 2019, **53**, 10070–10081.
14 B. S. Anderson, B. M. Phillips, J. P. Voorhees, K. Siegler and R. Tjeerdema, Bioswales reduce contaminants associated with toxicity in urban storm water, *Environ. Toxicol. Chem.*, 2016, **35**, 3124–3134.
15 A. Young, V. Kochenkov, J. K. McIntyre, J. D. Stark and A. B. Coffin, Urban stormwater runoff negatively impacts lateral line development in larval zebrafish and salmon embryos, *Sci. Rep.*, 2018, **8**, 2830.
16 C. Vignet, T. Cappello, Q. Fu, K. Lajoie, G. De Marco, C. Clérandeau, H. Mottaz, M. Maisano, J. Hollender, K. Schirmer and J. Cachot, Imidacloprid induces adverse effects on fish early life stages that are more severe in Japanese medaka (Oryzias latipes) than in zebrafish (Danio rerio), *Chemosphere*, 2019, **225**, 470–478.
17 Z. Tian, H. Zhao, K. T. Peter, M. Gonzalez, J. Wetzel, C. Wu, X. Hu, J. Prat, E. Mudrock, R. Hettinger, A. E. Cortina, R. G.

Biswas, F. V. C. Kock, R. Soong, A. Jenne, B. Du, F. Hou, H. He, R. Lundeen, A. Gilbreath, R. Sutton, N. L. Scholz, J. W. Davis, M. C. Dodd, A. Simpson, J. K. McIntyre and E. P. Kolodziej, A ubiquitous tire rubber–derived chemical induces acute mortality in coho salmon, *Science*, 2021, **371**, 185–189.

18 W. Mnif, A. I. H. Hassine, A. Bouaziz, A. Bartegi, O. Thomas and B. Roig, Effect of endocrine disruptor pesticides: a review, *Int. J. Environ. Res. Public Health*, 2011, **8**, 2265–2303.

19 C. Zhang, T. Schilirò, M. Gea, S. Bianchi, A. Spinello, A. Magistrato, G. Gilardi and G. Di Nardo, Molecular basis for endocrine disruption by pesticides targeting aromatase and estrogen receptor, *Int. J. Environ. Res. Public Health*, 2020, **17**, 5664.

20 R. Loos, G. Locoro, S. Comero, S. Contini, D. Schwesig, F. Werres, P. Balsaa, O. Gans, S. Weiss, L. Blaha, M. Bolchi and B. M. Gawlik, Pan-European survey on the occurrence of selected polar organic persistent pollutants in ground water, *Water Res.*, 2010, **44**, 4115–4126.

21 K. Kiefer, A. Müller, H. Singer and J. Hollender, New relevant pesticide transformation products in groundwater detected using target and suspect screening for agricultural and urban micropollutants with LC-HRMS, *Water Res.*, 2019, **165**, 114972.

22 A. B. Boehm, C. D. Bell, N. J. M. Fitzgerald, E. Gallo, C. P. Higgins, T. S. Hogue, R. G. Luthy, A. C. Portmann, B. A. Ulrich and J. M. Wolfand, Biochar-augmented biofilters to improve pollutant removal from stormwater–can they improve receiving water quality?, *Environ. Sci.: Water Res. Technol.*, 2020, **6**, 1520–1537.

23 K. Flanagan, P. Branchu, L. Boudahmane, E. Caupos, D. Demare, S. Deshayes, P. Dubois, L. Meffray, C. Partibane, M. Saad and M.-C. Gromaire, Field performance of two biofiltration systems treating micropollutants from road runoff, *Water Res.*, 2018, **145**, 562–578.

24 K. Zhang, A. Randelovic, D. Page, D. T. McCarthy and A. Deletic, The validation of stormwater biofilters for micropollutant removal using in situ challenge tests, *Ecol. Eng.*, 2014, **67**, 1–10.

25 R. Pitt, S. Clark and R. Field, Groundwater contamination potential from stormwater infiltration practices, *Urban Water*, 1999, **1**, 217–236.

26 T. R. Miles, E. M. Rasmussen and M. Gray, in *Agricultural and Environmental Applications of Biochar: Advances and Barriers*, Soil Science Society of America, Inc., Madison, WI, 2016, pp. 341–376.

27 B. A. Ulrich, E. A. Im, D. Werner and C. P. Higgins, Biochar and Activated Carbon for Enhanced Trace Organic Contaminant Retention in Stormwater Infiltration Systems, *Environ. Sci. Technol.*, 2015, **49**, 6222–6230.

28 J. R. Ray, I. A. Shabtai, M. Teixidó, Y. G. Mishael and D. L. Sedlak, Polymer-clay composite geomedia for sorptive removal of trace organic compounds and metals in urban stormwater, *Water Res.*, 2019, **157**, 454–462.

29 B. A. Ulrich, M. Loehnert and C. P. Higgins, Improved contaminant removal in vegetated stormwater biofilters amended with biochar, *Environ. Sci.: Water Res. Technol.*, 2017, **3**, 726–734.

30 F. Xiao and J. J. Pignatello, Interactions of triazine herbicides with biochar: Steric and electronic effects, *Water Res.*, 2015, **80**, 179–188.

31 M. Ahmad, A. U. Rajapaksha, J. E. Lim, M. Zhang, N. Bolan, D. Mohan, M. Vithanage, S. S. Lee and Y. S. Ok, Biochar as a sorbent for contaminant management in soil and water: A review, *Chemosphere*, 2014, **99**, 19–33.

32 M. L. Frankel, T. I. Bhuiyan, A. Veksha, M. A. Demeter, D. B. Layzell, R. J. Helleur, J. M. Hill and R. J. Turner, Removal and biodegradation of naphthenic acids by biochar and attached environmental biofilms in the presence of co-contaminating metals, *Bioresour. Technol.*, 2016, **216**, 352–361.

33 B. A. Ulrich, M. Vignola, K. Edgehouse, D. Werner and C. P. Higgins, Organic Carbon Amendments for Enhanced Biological Attenuation of Trace Organic Contaminants in Biochar-Amended Stormwater Biofilters, *Environ. Sci. Technol.*, 2017, **51**, 9184–9193.

34 W. K. Shieh and J. D. Keenan, Fluidized bed biofilm reactor for wastewater treatment, in *Bioproducts. Advances in Biochemical Engineering/Biotechnology*, Springer, Berlin, Heidelberg, 1986, vol 33, DOI: **10.1007/BFb0002455**.

35 J. A. Puhakka, E. S. Melin, K. T. Järvinen, P. M. Koro, J. A. Rintala, P. Hartikainen, W. K. Shieh and J. F. Ferguson, Fluidized-bed biofilms for chlorophenol mineralization, *Water Sci. Technol.*, 1995, **31**, 227–235.

36 K.-H. Oh and O. H. Tuovinen, Biodegradation of the phenoxy herbicides MCPP and 2,4-D in fixed-film column reactors, *Int. Biodeterior. Biodegrad.*, 1994, **33**, 93–99.

37 L. Hale, M. Luth and D. Crowley, Biochar characteristics relate to its utility as an alternative soil inoculum carrier to peat and vermiculite, *Soil Biol. Biochem.*, 2015, **81**, 228–235.

38 Y. Luo, M. Durenkamp, M. De Nobili, Q. Lin, B. J. Devonshire and P. C. Brookes, Microbial biomass growth, following incorporation of biochars produced at 350 °C or 700 °C, in a silty-clay loam soil of high and low pH, *Soil Biol. Biochem.*, 2013, **57**, 513–523.

39 R. S. Quilliam, H. C. Glanville, S. C. Wade and D. L. Jones, Life in the 'charosphere' – Does biochar in agricultural soil provide a significant habitat for microorganisms?, *Soil Biol. Biochem.*, 2013, **65**, 287–293.

40 J. M. Saquing, Y.-H. Yu and P. C. Chiu, Wood-Derived Black Carbon (Biochar) as a Microbial Electron Donor and Acceptor, *Environ. Sci. Technol. Lett.*, 2016, **3**, 62–66.

41 A. Kappler, M. L. Wuestner, A. Ruecker, J. Harter, M. Halama and S. Behrens, Biochar as an Electron Shuttle between Bacteria and Fe(III) Minerals, *Environ. Sci. Technol. Lett.*, 2014, **1**, 339–344.

42 L. Yu, Y. Yuan, J. Tang, Y. Wang and S. Zhou, Biochar as an electron shuttle for reductive dechlorination of pentachlorophenol by Geobacter sulfurreducens, *Sci. Rep.*, 2015, **5**, 16221.

43 J. Liu, Y. Ding, L. Ma, G. Gao and Y. Wang, Combination of biochar and immobilized bacteria in cypermethrin-contaminated soil remediation, *Int. Biodeterior. Biodegrad.*, 2017, **120**, 15–20.

44 Ö. Aktaş and F. Çeçen, Bioregeneration of activated carbon: A review, *Int. Biodeterior. Biodegrad.*, 2007, **59**, 257–272.
45 X. Tang, Y. Yang, R. Tao, P. Chen, Y. Dai, C. Jin and X. Feng, Fate of mixed pesticides in an integrated recirculating constructed wetland (IRCW), *Sci. Total Environ.*, 2016, **571**, 935–942.
46 Y. Yan, M. Ma, X. Liu, W. Ma, M. Li and L. Yan, Effect of biochar on anaerobic degradation of pentabromodiphenyl ether (BDE-99) by archaea during natural groundwater recharge with treated municipal wastewater, *Int. Biodeterior. Biodegrad.*, 2017, **124**, 119–127.
47 N. Ashoori, M. Teixido, S. Spahr, G. H. LeFevre, D. L. Sedlak and R. G. Luthy, Evaluation of pilot-scale biochar-amended woodchip bioreactors to remove nitrate, metals, and trace organic contaminants from urban stormwater runoff, *Water Res.*, 2019, **154**, 1–11.
48 M. Zhang, X. Shen, H. Zhang, D. Werner, B. Wang, Y. Yang, S. Tao and X. Wang, Humic Acid Can Enhance the Mineralization of Phenanthrene Sorbed on Biochars, *Environ. Sci. Technol.*, 2019, **53**, 13201–13208.
49 S. Kwon and J. J. Pignatello, Effect of Natural Organic Substances on the Surface and Adsorptive Properties of Environmental Black Carbon (Char): Pseudo Pore Blockage by Model Lipid Components and Its Implications for N2-Probed Surface Properties of Natural Sorbents, *Environ. Sci. Technol.*, 2005, **39**, 7932–7939.
50 J. J. Pignatello, S. Kwon and Y. Lu, Effect of Natural Organic Substances on the Surface and Adsorptive Properties of Environmental Black Carbon (Char): Attenuation of Surface Activity by Humic and Fulvic Acids, *Environ. Sci. Technol.*, 2006, **40**, 7757–7763.
51 A. Guillon, C. Videloup, C. Leroux, H. Bertin, M. Philibert, I. Baudin, A. Bruchet and M. Esperanza, Occurrence and fate of 27 triazines and metabolites within French drinking water treatment plants, *Water Supply*, 2018, **19**, 463–471.
52 C. Hao, M. R. Noestheden, X. Zhao and D. Morse, Liquid chromatography–tandem mass spectrometry analysis of neonicotinoid pesticides and 6-chloronicotinic acid in environmental water with direct aqueous injection, *Anal. Chim. Acta*, 2016, **925**, 43–50.
53 C. P. Muerdter and G. H. LeFevre, Synergistic Lemna Duckweed and Microbial Transformation of Imidacloprid and Thiacloprid Neonicotinoids, *Environ. Sci. Technol. Lett.*, 2019, **6**, 761–767.
54 E. L. Schymanski, J. Jeon, R. Gulde, K. Fenner, M. Ruff, H. P. Singer and J. Hollender, Identifying Small Molecules via High Resolution Mass Spectrometry: Communicating Confidence, *Environ. Sci. Technol.*, 2014, **48**, 2097–2098.
55 J. E. Grebel, J. A. Charbonnet and D. L. Sedlak, Oxidation of organic contaminants by manganese oxide geomedia for passive urban stormwater treatment systems, *Water Res.*, 2016, **88**, 481–491.
56 X. Gu, T. F. M. Rodgers, S. Spraakman, T. Van Seters, R. Flick, M. L. Diamond, J. Drake and E. Passeport, Trace Organic Contaminant Transfer and Transformation in Bioretention Cells: A Field Tracer Test with Benzotriazole, *Environ. Sci. Technol.*, 2021, **55**, 12281–12290.
57 D. Werner, U. Ghosh and R. G. Luthy, Modeling Polychlorinated Biphenyl Mass Transfer after Amendment of Contaminated Sediment with Activated Carbon, *Environ. Sci. Technol.*, 2006, **40**, 4211–4218.
58 D. Werner, H. K. Karapanagioti and D. A. Sabatini, Assessing the effect of grain-scale sorption rate limitations on the fate of hydrophobic organic groundwater pollutants, *J. Contam. Hydrol.*, 2012, **129**, 70–79.
59 C. J. Liu, D. Werner and C. Bellona, Removal of per- and polyfluoroalkyl substances (PFASs) from contaminated groundwater using granular activated carbon: a pilot-scale study with breakthrough modeling, *Environ. Sci.: Water Res. Technol.*, 2019, **5**, 1844–1853.
60 X. Yu, Z. Qi, X. Zhang, P. Yu, B. Liu, L. Zhang and L. Fu, Nitrogen loss and oxygen paradox in full-scale biofiltration for drinking water treatment, *Water Res.*, 2007, **41**, 1455–1464.
61 L. Sbardella, J. Comas, A. Fenu, I. Rodriguez-Roda and M. Weemaes, Advanced biological activated carbon filter for removing pharmaceutically active compounds from treated wastewater, *Sci. Total Environ.*, 2018, **636**, 519–529.
62 S. S. Dalahmeh, N. Alziq and L. Ahrens, Potential of biochar filters for onsite wastewater treatment: Effects of active and inactive biofilms on adsorption of per- and polyfluoroalkyl substances in laboratory column experiments, *Environ. Pollut.*, 2019, **247**, 155–164.
63 N. Klimenko, S. Smolin, S. Grechanyk, V. Kofanov, L. Nevynna and L. Samoylenko, Bioregeneration of activated carbons by bacterial degraders after adsorption of surfactants from aqueous solutions, *Colloids Surf., A*, 2003, **230**, 141–158.
64 V. Abromaitis, V. Racys, P. van der Marel and R. J. W. Meulepas, Biodegradation of persistent organics can overcome adsorption–desorption hysteresis in biological activated carbon systems, *Chemosphere*, 2016, **149**, 183–189.
65 X.-Y. Yu, G.-G. Ying and R. S. Kookana, Sorption and Desorption Behaviors of Diuron in Soils Amended with Charcoal, *J. Agric. Food Chem.*, 2006, **54**, 8545–8550.
66 J.-L. Bertrand-Krajewski, G. Chebbo and A. Saget, Distribution of pollutant mass vs volume in stormwater discharges and the first flush phenomenon, *Water Res.*, 1998, **32**, 2341–2356.
67 P. M. Bach, D. T. McCarthy and A. Deletic, Redefining the stormwater first flush phenomenon, *Water Res.*, 2010, **44**, 2487–2498.
68 K. T. Peter, F. Hou, Z. Tian, C. Wu, M. Goehring, F. Liu and E. P. Kolodziej, More Than a First Flush: Urban Creek Storm Hydrographs Demonstrate Broad Contaminant Pollutographs, *Environ. Sci. Technol.*, 2020, **54**, 6152–6165.
69 H. Lee, S.-L. Lau, M. Kayhanian and M. K. Stenstrom, Seasonal first flush phenomenon of urban stormwater discharges, *Water Res.*, 2004, **38**, 4153–4163.

70 U. Ogbonnaya and K. T. Semple, Impact of biochar on organic contaminants in soil: a tool for mitigating risk?, *Agronomy*, 2013, **3**, 349–375.
71 Y. Ogata, T. Toyama, N. Yu, X. Wang, K. Sei and M. Ike, Occurrence of 4-tert-butylphenol (4-t-BP) biodegradation in an aquatic sample caused by the presence of Spirodela polyrrhiza and isolation of a 4-t-BP-utilizing bacterium, *Biodegradation*, 2013, **24**, 191–202.
72 P. Zhang, H. Sun, L. Yu and T. Sun, Adsorption and catalytic hydrolysis of carbaryl and atrazine on pig manure-derived biochars: Impact of structural properties of biochars, *J. Hazard. Mater.*, 2013, **244**, 217–224.
73 S.-Y. Oh, J.-G. Son and P. C. Chiu, Biochar-mediated reductive transformation of nitro herbicides and explosives, *Environ. Toxicol. Chem.*, 2013, **32**, 501–508.
74 A. Mudhoo and V. K. Garg, Sorption, Transport and Transformation of Atrazine in Soils, Minerals and Composts: A Review, *Pedosphere*, 2011, **21**, 11–25.
75 A. H. Meyer, H. Penning and M. Elsner, C and N Isotope Fractionation Suggests Similar Mechanisms of Microbial Atrazine Transformation Despite Involvement of Different Enzymes (AtzA and TrzN), *Environ. Sci. Technol.*, 2009, **43**, 8079–8085.
76 L. Wackett, M. Sadowsky, B. Martinez and N. Shapir, Biodegradation of atrazine and related s-triazine compounds: from enzymes to field studies, *Appl. Microbiol. Biotechnol.*, 2002, **58**, 39–45.
77 J. F. Douglass, M. Radosevich and O. H. Tuovinen, Mineralization of atrazine in the river water intake and sediments of a constructed flow-through wetland, *Ecol. Eng.*, 2014, **72**, 35–39.
78 D. A. Thompson, H.-J. Lehmler, D. W. Kolpin, M. L. Hladik, J. D. Vargo, K. E. Schilling, G. H. LeFevre, T. L. Peeples, M. C. Poch, L. E. LaDuca, D. M. Cwiertny and R. W. Field, A critical review on the potential impacts of neonicotinoid insecticide use: current knowledge of environmental fate, toxicity, and implications for human health, *Environ. Sci.: Processes Impacts*, 2020, **22**, 1315–1346.
79 M. Tomizawa and J. E. Casida, Selective toxicity of neonicotinoids attributable to specificity of insect and mammalian nicotinic receptors, *Annu. Rev. Entomol.*, 2003, **48**, 339–364.
80 R. Nauen, U. Reckmann, S. Armborst, H.-P. Stupp and A. Elbert, Whitefly-active metabolites of imidacloprid: biological efficacy and translocation in cotton plants, *Pestic. Sci.*, 1999, **55**, 265–271.
81 S. Suchail, D. Guez and L. P. Belzunces, Discrepancy between acute and chronic toxicity induced by imidacloprid and its metabolites in Apis mellifera, *Environ. Toxicol. Chem.*, 2001, **20**, 2482–2486.
82 J.-M. Bonmatin, C. Giorio, V. Girolami, D. Goulson, D. P. Kreutzweiser, C. Krupke, M. Liess, E. Long, M. Marzaro, E. A. D. Mitchell, D. A. Noome, N. Simon-Delso and A. Tapparo, Environmental fate and exposure; neonicotinoids and fipronil, *Environ. Sci. Pollut. Res.*, 2015, **22**, 35–67.
83 S. Hussain, C. J. Hartley, M. Shettigar and G. Pandey, Bacterial biodegradation of neonicotinoid pesticides in soil and water systems, *FEMS Microbiol. Lett.*, 2016, **363**(23), fnw252.
84 O. Malev, R. S. Klobučar, E. Fabbretti and P. Trebše, Comparative toxicity of imidacloprid and its transformation product 6-chloronicotinic acid to non-target aquatic organisms: Microalgae Desmodesmus subspicatus and amphipod Gammarus fossarum, *Pestic. Biochem. Physiol.*, 2012, **104**, 178–186.
85 T. Van der Velde-Koerts, P. H. Van Hoeven-Arentzen and C. M. Mahieu, *Clothianidin (238). Pesticide Residues in Food 2010: Evaluations Part I-Residues; FAO Plant Production and Protection Paper 206.*, World Health Organization & Food and Agriculture Organization of the United States, Rome, 2011.
86 T. Mori, J. Wang, Y. Tanaka, K. Nagai, H. Kawagishi and H. Hirai, Bioremediation of the neonicotinoid insecticide clothianidin by the white-rot fungus Phanerochaete sordida, *J. Hazard. Mater.*, 2017, **321**, 586–590.
87 P. Zhang, C. Ren, H. Sun and L. Min, Sorption, desorption and degradation of neonicotinoids in four agricultural soils and their effects on soil microorganisms, *Sci. Total Environ.*, 2018, **615**, 59–69.
88 R. A. Mulligan, P. L. Tomco, M. W. Howard, T. T. Schempp, D. J. Stewart, P. M. Stacey, D. B. Ball and R. S. Tjeerdema, Aerobic versus Anaerobic Microbial Degradation of Clothianidin under Simulated California Rice Field Conditions, *J. Agric. Food Chem.*, 2016, **64**, 7059–7067.
89 K. L. Klarich, N. C. Pflug, E. M. DeWald, M. L. Hladik, D. W. Kolpin, D. M. Cwiertny and G. H. LeFevre, Occurrence of Neonicotinoid Insecticides in Finished Drinking Water and Fate during Drinking Water Treatment, *Environ. Sci. Technol. Lett.*, 2017, **4**, 168–173.
90 W. L. Desiante, N. S. Minas and K. Fenner, Micropollutant biotransformation and bioaccumulation in natural stream biofilms, *Water Res.*, 2021, **193**, 116846.
91 C. Seller, M. Honti, H. Singer and K. Fenner, Biotransformation of Chemicals in Water–Sediment Suspensions: Influencing Factors and Implications for Persistence Assessment, *Environ. Sci. Technol. Lett.*, 2020, **7**, 854–860.
92 P. Zhang, H. Sun, C. Ren, L. Min and H. Zhang, Sorption mechanisms of neonicotinoids on biochars and the impact of deashing treatments on biochar structure and neonicotinoids sorption, *Environ. Pollut.*, 2018, **234**, 812–820.
93 M. Kah, G. Sigmund, F. Xiao and T. Hofmann, Sorption of ionizable and ionic organic compounds to biochar, activated carbon and other carbonaceous materials, *Water Res.*, 2017, **124**, 673–692.
94 M. Tomizawa, N. Zhang, K. A. Durkin, M. M. Olmstead and J. E. Casida, The Neonicotinoid Electronegative Pharmacophore Plays the Crucial Role in the High Affinity and Selectivity for the Drosophila Nicotinic Receptor: An Anomaly for the Nicotinoid Cation–π Interaction Model, *Biochemistry*, 2003, **42**, 7819–7827.

95 D. T. Webb, M. R. Nagorzanski, M. M. Powers, D. M. Cwiertny, M. L. Hladik and G. H. LeFevre, Differences in Neonicotinoid and Metabolite Sorption to Activated Carbon Are Driven by Alterations to the Insecticidal Pharmacophore, *Environ. Sci. Technol.*, 2020, **54**, 14694–14705.

96 F. Xiao and J. J. Pignatello, π+–π Interactions between (Hetero)aromatic Amine Cations and the Graphitic Surfaces of Pyrogenic Carbonaceous Materials, *Environ. Sci. Technol.*, 2015, **49**, 906–914.

97 F. Menger, G. Boström, O. Jonsson, L. Ahrens, K. Wiberg, J. Kreuger and P. Gago-Ferrero, Identification of Pesticide Transformation Products in Surface Water Using Suspect Screening Combined with National Monitoring Data, *Environ. Sci. Technol.*, 2021, **55**, 10343–10353.

98 D. T. Webb, M. R. Nagorzanski, D. M. Cwiertny and G. H. LeFevre, Combining Experimental Sorption Parameters with QSAR to Predict Neonicotinoid and Transformation Product Sorption to Carbon Nanotubes and Granular Activated Carbon, *ACS ES&T Water*, 2022, **2**, 247–258.

99 C. E. Schaefer, D. M. Drennan, D. N. Tran, R. Garcia, E. Christie, C. P. Higgins and J. A. Field, Measurement of Aqueous Diffusivities for Perfluoroalkyl Acids, *J. Environ. Eng.*, 2019, **145**, 6019006.

100 R. Sutton, Y. Xie, K. D. Moran and J. Teerlink, in *Pesticides in Surface Water: Monitoring, Modeling, Risk Assessment, and Management*, American Chemical Society, 2019, vol. 1308, pp. 5–63.

101 P. M. Bradley, C. A. Journey, K. M. Romanok, L. B. Barber, H. T. Buxton, W. T. Foreman, E. T. Furlong, S. T. Glassmeyer, M. L. Hladik, L. R. Iwanowicz, D. K. Jones, D. W. Kolpin, K. M. Kuivila, K. A. Loftin, M. A. Mills, M. T. Meyer, J. L. Orlando, T. J. Reilly, K. L. Smalling and D. L. Villeneuve, Expanded Target-Chemical Analysis Reveals Extensive Mixed-Organic-Contaminant Exposure in U.S. Streams, *Environ. Sci. Technol.*, 2017, **51**, 4792–4802.

102 K. M. Spahr, C. D. Bell, J. E. McCray and T. S. Hogue, Greening up stormwater infrastructure: Measuring vegetation to establish context and promote cobenefits in a diverse set of US cities, *Urban For. Urban Green*, 2020, **48**, 126548.

103 V. Venkataramanan, A. I. Packman, D. R. Peters, D. Lopez, D. J. McCuskey, R. I. McDonald, W. M. Miller and S. L. Young, A systematic review of the human health and social well-being outcomes of green infrastructure for stormwater and flood management, *J. Environ. Manage.*, 2019, **246**, 868–880.

